Decay of superfluid currents in a moving system of strongly interacting bosons

A. Polkovnikov, E. Altman, E. Demler, B. Halperin, and M. D. Lukin
Physics Department, Harvard University, Cambridge, Massachusetts 02138, USA
(Received 20 December 2004; published 23 June 2005)

We analyze the stability and decay of supercurrents of strongly interacting bosons on optical lattices. At the mean-field level, the system undergoes an irreversible dynamic phase transition, whereby the current decays beyond a critical phase gradient that depends on the interaction strength. At commensurate filling the transition line smoothly interpolates between the classical modulational instability of weakly interacting bosons and the equilibrium Mott transition at zero current. Below the mean-field instability, the current can decay due to quantum and thermal phase slips. We derive asymptotic expressions of the decay rate near the critical current. In a three-dimensional optical lattice this leads to very weak broadening of the transition. In one and two dimensions the broadening leads to significant current decay well below the mean-field critical current. We show that the temperature scale below which quantum phase slips dominate the decay of supercurrents is easily within experimental reach.

DOI: 10.1103/PhysRevA.71.063613 PACS number(s): 03.75.Lm, 03.75.Kk

I. INTRODUCTION

Many-body physics of strongly interacting ultracold atoms in optical lattices has been actively explored in the recent years [1]. In particular, quantum effects of strongly interacting bosons, such as number squeezed states generation [2] and a quantum phase transition from the superfluid to the Mott insulator [3], have been observed in agreement with earlier theoretical predictions [4,5]. These developments were followed by a broader theoretical analysis of phase diagrams of more complex systems including multicomponent bosons [6–9], Bose-Fermi mixtures [10–12], and exotic states exhibiting topological orders [13,14]. Such studies are motivated by issues that arise in a traditional condensed-matter context. However, unique features of the cold atom systems also raise a completely new set of questions. In particular, the ability to continuously vary interaction parameters, coupled to the near perfect isolation of these systems, opens the way to address quantum dynamics far from equilibrium.

In this context, there exists a purely dynamical phase transition of a condensate of weakly interacting bosons moving in an optical lattice. If the wave vector associated with the condensate momentum exceeds a critical value, which is equal to one-quarter of the reciprocal-lattice constant for the square lattice [15,16], then the coherent motion of the condensate becomes unstable, resulting in the loss of superfluidity. Such a dynamical instability was observed experimentally [17] by measuring loss of coherence as a function of the condensate momentum. This transition is of classical origin, in the sense that it is seen as an instability in the Gross-Pitaveskii equations of motion (GPE). Reltaed nonlinear dynamical phenomena such as self-trapping and soliton formation have been studied in theory and experiment [18–21]. However, these studies focused on essentially classical systems, well described by GPE. Very little progress has been made in analyzing far from equilibrium behavior of systems where strong interactions and quantum fluctuations play an important role.

In the present work we address this issue by focusing on a problem relevant to recent experiments: the fate of superfluid currents in optical lattices in the strongly interacting regime. We shall consider this issue via two questions, which will turn out to be closely related. First, what is the effect of quantum (as well as thermal) fluctuations on the dynamical instability of a moving condensate? May the instabilitiy occur earlier, for example, in this case than the GPE prediction of $p_c=\pi/2$? The second question is, how does the superfluid–to–Mott-insulator transition take place when the condensate is moving in the lattice. This question may have direct relevance for ongoing experiments on the superfluid-insulator transition. When the condensate is loaded into a magnetic trap it is hard to completely avoid center-of-mass oscillations. In the absence of the optical lattice such a motion is frictionless and can persist for very long times. The same is true in the superfluid phase in the presence of the optical lattice as long as the center-of-mass momentum remains small and the interactions are weak. But what is the ultimate fate of this motion as the optical potential is increased and the system approaches the insulating regime?

Effect of weak quantum fluctuations on the modulational instability in one-dimensional traps was analyzed earlier numerically by one of us [22]. It was shown that the quantum fluctuations smoothen the sharp classical transition and lead to the current decay at smaller amplitude of the center-of-mass oscillations than predicted using the classical Gross-Pitaevskii (GP) equations alone. Similar numerical results were also reported in Ref. [23]. Recent experiments confirmed strong damping of the center-of-mass oscillations in one-dimensional condensates far from the classical modulational instability [24].

In this paper we present a general theoretical framework of a superfluid-insulator transition in the current carrying state. Strictly speaking this is a true phase transition only at zero current. However, we find regimes where the broadening of the transition is small and even where a true discontinuity survives. In such cases a phase boundary is still well defined.

We shall show that at any nonzero current the transition is irreversible. If one starts from a condensate with nonzero current, increases the lattice strength past the transition point,

then decreases it back to the original state, the current in the final state will have vanished. The energy contained in the initial motion of the condensate is transferred into thermal incoherent excitations. Thus the dynamical transition is of the first-order type. The current carrying state is a metastable minimum of the classical (saddle-point) energy, and the transition occurs when the system escapes from this state.

Throughout this work we employ the well-known boson Hubbard model [25], described by the Hamiltonian

$$\mathcal{H} = \sum_{\langle jk \rangle} -J(a_j^\dagger a_k + a_k^\dagger a_j) + \sum_j \frac{U}{2} a_j^\dagger a_j (a_j^\dagger a_j - 1), \qquad (1)$$

where $a_j^\dagger$ and a_j are the boson creation and annihilation operators at the lattice site j, $\langle jk \rangle$ denotes pairs of nearest neighbors, J is the single-particle hopping amplitude, and U is the on-site repulsive interaction. Another implicit parameter is the average number of bosons per site N. If also a condition $UN \gg J$ is fulfilled, then the boson Hubbard model can be mapped into the O(2) quantum rotor model [25]:

$$\mathcal{H} = \sum_{\langle jk \rangle} -2JN \cos(\phi_k - \phi_j) + \sum_j \frac{U}{2} n_j^2, \qquad (2)$$

where ϕ_j and n_j are the conjugate phase and the number of particles on the site j. The system described by Eq. (2) also undergoes a superfluid insulator transition at $JN \sim U$ and can support current in the superfluid phase. In many situations, the quantum rotor model is easier to analyze analytically and we will frequently appeal to it. It is usually well justified in the case $N \gg 1$. Indeed, in this limit it is possible to have simultaneously $UN \gg J$ and JN either smaller or larger than U. So at large N the mapping from the boson Hubbard to the quantum rotor model can be justified in both the superfluid and insulating phases.

Our paper is organized as follows. In Sec. II we give an overview of our main results and present a physical picture. In Sec. III we derive the mean-field phase diagram separating stable and unstable regimes of current flow. Section IV focuses on the current decay mechanisms due to quantum and thermal fluctuations. In particular, we obtain leading asymptotic contributions to both quantum and thermal decay rates near the mean-field instability. Then in Sec. V we consider dynamics of the current decay and discuss the effects of a parabolic confining potential. Section VI addresses the loss of coherence in a condensate following supercurrent decay. In Sec. VII we present the results of exact simulations in small systems and discuss them in the context of our theoretical analysis. Finally, in Sec. VIII we summarize the results and discuss experimental implications. A shorter discussion of the results presented here can be found in Ref. [26].

II. PHYSICAL PICTURE AND OVERVIEW OF THE RESULTS

The existence of a critical velocity of a condensate in an optical lattice was predicted [15,16] and observed experimentally [17,18] in the regime of weak quantum fluctuations ($JN \gg U$). In this case one can solve the Gross-Pitaevskii equations of motion and find that the condensate becomes unstable when the phase difference between adjacent sites becomes larger than $\pi/2$. There is a simple way to understand this instability by considering how the superfluid current flowing through the system changes with the condensate momentum. In a continuum system the current is just

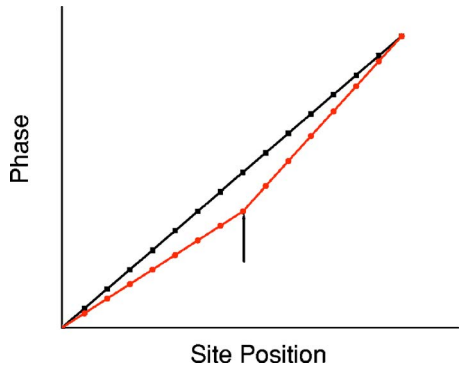

FIG. 1. Schematic representation of a perturbation to a state with a uniform phase gradient. Dots represent phases on different sites for uniform and perturbed systems. The lines are guides to the eye.

$$\mathcal{J} = \rho_s p, \qquad (3)$$

where ρ_s denotes the superfluid density and p the momentum or phase gradient such that $\phi(x) = px$. In a discrete system described by a tight-binding model, the above expression is modified to

$$\mathcal{J} = \rho_s \sin p. \qquad (4)$$

More generally $\sin p$ is replaced by a different function of p, with the same elementary period. At small currents we recover the continuum limit from Eq. (4). In the Gross-Pitaevskii regime, the superfluid density does not depend on momentum. Therefore the maximal current occurs at $p = \pi/2$, precisely where the condensate motion becomes unstable. As we argue below, this is not a coincidence. Consider a perturbation, where the state with a uniform phase gradient p is split into two equal domains with slightly higher and slightly lower momenta $p \pm \delta p$ (see Fig. 1). At small δp we can expand the energy difference between the perturbed and unperturbed configurations in powers of δp. The linear term in the expansion vanishes because the contributions to the energy from the left and the right domains exactly cancel each other and we are left only with the quadratic term:

$$\delta E \approx \frac{1}{2}\frac{dE}{dp}\delta p + \frac{1}{2}\frac{dE}{dp}(-\delta p) + 2\frac{1}{4}\frac{d^2E}{dp^2}(\delta p)^2 = \frac{1}{2}\frac{d^2E}{dp^2}(\delta p)^2. \qquad (5)$$

Noting that the superfluid current is formally defined as the derivative of the energy with respect to phase gradient, $\mathcal{J}(p) = dE/dp$, we find

$$\delta E \propto \frac{d\mathcal{J}}{dp}(\delta p)^2. \tag{6}$$

Thus if the current is an increasing function of the momentum, then small deviations from the uniform state increase its energy. On the other hand, if $d\mathcal{J}/dp<0$ then the fluctuation just considered reduces the energy of the system. In this case it is obvious there is a manifold of resonant configurations obtained by a smooth continuum transformation from a uniform state. For example, one can take the state in Fig. 1 plus a weak positive energy fluctuation. So there is no energy barrier protecting a uniform state from fragmentation. Let us note that this argument shows that the positive slope of the current with respect to p is a necessary condition for the stability of the uniform state. It does not exclude, however, that the current can decay even if this condition is satisfied. In Sec. IV we will see that this indeed occurs due to quantum or thermal phase slips [27,28].

Consider now the strongly interacting regime. Suppose that we deal with a uniform system at commensurate (i.e., integer) filling. It is well known that such systems undergo a superfluid-insulator transition [4] at zero temperature. This transition is driven by quantum fluctuations which increase with the interaction strength. As p increases the effective hopping amplitude in the direction parallel to the current decreases as $J_{\mathrm{eff}}\rightarrow J\cos p$ resulting in reduction of the sound velocity [16]. Alternatively, reduction of J_{eff} can be viewed as an increase of the single-particle effective mass with quasimomentum. This immediately follows from a single-particle band structure. As a result, quantum fluctuations, which are determined by the ratio $(U/J_{\mathrm{eff}}N)$ [35], become stronger with p, implying concomitant increase of quantum depletion of the superfluid density. Therefore Eq. (4) should be rewritten as

$$\mathcal{J}=\rho(p)\sin p, \tag{7}$$

where $\rho(p)$ is a monotonically decreasing function of the momentum. Thus the product reaches a maximum at some $p^{\star}<\pi/2$. In the Gross-Pitaevskii regime $JN\gg U$, the dependence of $\rho(p)$ on p is very weak and we find that $p^{\star}\approx\pi/2$. On the other hand, in the vicinity of the superfluid-insulator transition $\rho(p)$ is both very small and very sensitive to variations of J_{eff}. Thus we expect that in this case $p^{\star}$ will be close to zero.

In Sec III we give a formal derivation of the critical momentum at which the condensate motion becomes unstable. Using the time-dependent Gutzwiller approximation, we plot the critical momentum as a function of the interaction strength. This phase boundary interpolates between the usual dynamical instability occurring at $p=\pi/2$ for small interactions and the vanishing critical momentum at the equilibrium superfluid-insulator (SF-IN) transition (see the top graph in Fig. 4).

The situation is different in the noncommensurate case. No matter how strong the interaction strength, it cannot localize the excess particles (or holes) moving on top of the Mott background. This excess density always remains superfluid, independent of J_{eff} and thus also of p. Together with Eq. (7), this implies that at strong interactions the instability occurs at $p=\pi/2$. On the other hand, for sufficiently weak interactions, where the number fluctuation per site $\delta N\gg 1$, there is no distinction between integer and noninteger density. Therefore for U not too large the critical momentum should decrease with U from $\pi/2$. Indeed we find, using the time-dependant Gutzwiller approximation, that for the incommensurate case p_c reaches a minimum at some finite interaction strength and saturates on $\pi/2$ for both very weak and very strong interactions (see the bottom graph in Fig. 4).

In Sec. III B we develop an analytical approach, which describes the behavior of the critical momentum p_c versus interaction in the vicinity of the zero-current SF-IN transition. We show that in the commensurate case p_c vanishes as $1/\xi$, where ξ is a coherence length, which diverges at the transition. At noninteger filling we confirm the nonmonotonic behavior of the critical momentum.

In practice the system always includes a global harmonic confinement, which leads to a nonuniform density distribution. In this case we find that the instability first occurs at the the edges of the condensate where $N=1$ regardless of the peak density N_0 in the middle of the trap (see Sec. V). There is a difference between large and small N_0, which manifests in the dynamics of the current decay. For $N_0\approx 1$ (as well as in uniform systems with arbitrary filling) we find that near the instability the decay is underdamped, i.e., the instability rapidly grows in time destroying the current state. On the other hand, if N_0 is large, the momentum oscillations decay gradually after the edges become unstable. There is another important difference between the uniform and parabolically trapped condensates. In a uniform lattice there are only two energy scales, set by U and J, and their ratio completely determines the behavior of the system. With harmonic confinement on the other hand, due to the presence of another energy scale one should take into consideration whether U or J or both are being changed in the experiment (see the discussion in Sec. V and Appendix C).

So far we concentrated on the results of the mean-field dynamics at zero temperature, where the time evolution is simply described by classical equations of motion. In Sec. IV we go beyond the mean-field dynamics to analyze the effect of quantum and thermal fluctuations. These act to generate phase slips, which induce current decay even prior to the classical instability. A phase configuration for a particular phase slip is shown in Fig. 2. Basically a phase slip corresponds to generation of a large phase difference on a particular link (or in the vicinity of this link) and simultaneous reduction of the phase gradient in the rest of the chain. Because the energy is a periodic function of phase differences, by generating phase slips the system reduces its superfluid current. We calculate the leading exponents of the decay rates in the Gross-Pitaevskii regime of relatively weak interactions and in the quantum critical regime close to the SF-IN transition. We find that broadening of the mean-field transition is strongest in the one-dimensional case. In particular, deep in the superfluid regime, the phase-slip tunneling rate at $p\rightarrow\pi/2$ scales as

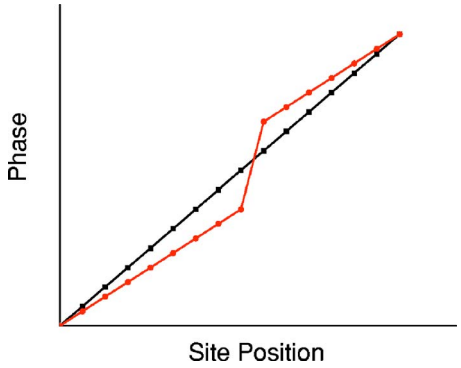

FIG. 2. Schematic representation of a phase slip. Notations are the same as in Fig. 1.

$$\Gamma \propto \exp\left(-S_d\sqrt{\frac{JN}{U}}(\pi/2-p)^{(6-d/2)}\right), \tag{8}$$

where S_d is just a number that depends on the number of space dimensions [see Eqs. (50)–(52)]. We obtain similar results for the thermal decay. Although below $\pi/2$ the decay in three dimensions is clearly much weaker than in one dimension, there is no qualitative difference between various dimensions. As long as the ratio JN/U remains large, the tunneling of phase slips is exponentially suppressed.

Next we derive analytical expressions for the exponents characterizing the decay rate in the vicinity of the equilibrium SF-IN transition. We find again that fluctuation induced decay is stronger in lower dimensions. However, there is no small parameter like U/JN controlling the mean-field results. We show that in one dimension the exponent always remains of the order of 1, implying significant broadening of the mean-field transition. In three dimensions, by contrast, we find that the quantum decay rate does not vanish at the mean-field instability, but rather exhibits a discontinuous jump. In this sense, the three-dimensional system undergoes a sharp dynamical transition at zero temperature.

The physical picture of current decay due to generation of phase slips is similar to the situation in superconductors. In particular, deviation of the critical current from the mean-field result was observed in thin superconducting wires [29] and explained theoretically [30,31]. The mechanism responsible for reduction of the critical current was identified as creation of phase slips due to thermal fluctuations. The question of observing current decay in superconductors due to quantum tunneling is still debated (see Ref. [27] for recent developments). We will show that in the systems under consideration here, current decay due to quantum effects is easily within experimentally reach. For a one-dimensional system, for example, the characteristic temperature below which quantum decay dominates in the GP regime (far from the Mott transition) is of the order of the Josephson energy ($T^\star \approx \sqrt{UJN}$). This is much higher than typical temperatures in optical lattice experiments. At strong interactions, in the vicinity of the Mott transition, broadening of the mean-field transition due to quantum phase slips is always large in one and two dimensions. Only in the three-dimensional case, where quantum tunneling is suppressed, can thermal fluctuations be responsible for current decay below the mean-field transition. Some additional details on the relation between current decay in superconductors and in optical lattices can be found in Ref. [32].

Let us now briefly mention some interesting experimental implications of our results. We envision the following experimental scheme. Start with a superfluid state far from the Mott insulator. Then either boost the condensate to some nonzero momentum [17], or induce a center-of-mass oscillation in the trap [24]. Now, slowly increase the interaction parameter up to a specified point. This can be done in the usual way by increasing the lattice intensity, or alternatively by decreasing the detuning from a Feshbach resonance. Finally decrease the interactions back to their original value. If the dynamical phase transition is sharp then as long as the system does not cross the transition boundary [Fig. 4(a)] within this cycle, the process should be completely reversible. In particular, the initial current (or center-of-mass oscillation), as well as phase coherence, should be fully recovered. At the same time, if the system does pass through the transition, the current will be lost irreversibly and the system will heat and partially lose its coherence, compared to the original state.

One of our main results is that in a three-dimensional optical lattice this mean-field dynamical transition is sharp, and it essentially survives the effect of fluctuations. Such experiments can thus map the nonequilibrium phase diagram shown in (Fig. 4) and directly trace the connection between the classical modulational instability ($p_c=\pi/2$) and the the equilibrium Mott transition. In fact, due to its discontinuous nature, the dynamical transition point is much easier to detect. This suggests an accurate method to determine the position of the equilibrium Mott transition by extrapolating the dynamical transition line to zero momentum.

One comment is in order concerning heating and loss of coherence in the final state. In Sec. VI we show that in three dimensions this loss of coherence is only significant at very large currents ($p\sim\pi/2$). In one dimension (and to a lesser extent in two dimensions), the loss of coherence due to irreversible heating depends on the system size or experimental resolution and may thus be large even at small currents.

III. MEAN-FIELD DYNAMICS AND CRITICAL CURRENTS IN OPTICAL LATTICES

A. Gross-Pitaveskii regime

Despite its simple form, the Bose Hubbard model (1) is not integrable in any spatial dimension [33,34] and cannot be solved completely. Nevertheless, there are some limits where one can make considerable progress in understanding its static and dynamic properties. In particular, one can easily address the regime of weak quantum fluctuations, which is the case when $JN \gg U$ [35]. Then one can use discrete Gross-Pitaveskii equations [36]. For the Hamiltonian (1) these are given by

$$i\frac{d\psi_j}{dt} = -J\sum_{k\in O}\psi_k + U|\psi_j|^2\psi_j, \tag{9}$$

where the classical fields ψ_j and $\psi_j^\star$ correspond to the expectation values of a_j and $a_j^\dagger$, respectively; the set O contains the

nearest neighbors of site j. In the quantum rotor limit $UN \gg J$ the number fluctuations are weak and can be integrated out leaving us with equations of motion for the phase $\phi_j = \arg \psi_j$ only:

$$\frac{d^2\phi_j}{dt^2} = -2UJN \sum_{k \in O} \sin(\phi_k - \phi_j). \tag{10}$$

Both Eqs. (9) and (10) can support stationary current carrying states $\psi_j \propto \exp(ipj)$. A simple linear stability analysis shows that these states are stable towards small perturbations for $p < \pi/2$ and become unstable otherwise [15,16]. Thus $\pi/2$ is the critical phase twist above which a uniform superfluid state breaks down. The transition from the superfluid to the insulating state associated with this instability is known as the classical localization transition. It was recently observed experimentally [17]. In the presence of quantum fluctuations, the current can decay even for $p < \pi/2$ via quantum tunneling. Clearly these fluctuations should be increasingly important as the system approaches the Mott phase. The same is true for decay due to thermal fluctuations as one increases the temperature. In the next section we will address this issue in detail.

B. Critical current in the vicinity of the SF-IN transition

The Gross-Pitaveskii description of the dynamics breaks down at strong interactions. Moreover, when $JN \sim U$ the Bosonic system at commensurate filling (N is integer) undergoes the Mott insulator transition entirely driven by quantum fluctuations [4,25]. In the uniform system with a fixed density this transition lies in the universality class of the xy model in $d+1$ dimensions [25], the properties of which were well studied long ago [37]. So there is also hope to get insights to some nonequilibrium properties of the interacting bosons in the vicinity of the phase transition. The latter, as any generic second-order phase transition, is characterized by a diverging correlation length ξ [25], which sets the length scale for all low-energy universal properties of the system. In particular, close to the critical point the low-energy long-wavelength fluctuations can be described by relativistic ($z=1$) effective field theory [25]. In terms of dynamics this implies that the classical equations of motion also take explicitly relativistic invariant form [38]:

$$\frac{\partial^2\psi}{\partial t^2} = \nabla^2\psi + r\psi - |\psi|^2\psi, \tag{11}$$

where ψ is the superfluid order parameter, r tunes the system across the SF-IN transition: $r>0$ corresponds to the superfluid phase and $r<0$ does to the insulator. Here we rescaled the units of coordinates and time by a constant of the order of 1 (see Appendix A for the details). The correlation length ξ is related to the tuning parameter r as $\xi \propto 1/\sqrt{|r|}$. We point out that Eq. (11) is very reminiscent of the conventional continuum Gross-Pitaeskii equation with the only difference that there is a second- (as opposed to first-) order time derivative in the left-hand side. This equation has a conserved charge:

$$Q = \int d^dx \frac{A}{2i}(\psi^* \partial_t \psi - \psi \partial_t \psi^*), \tag{12}$$

which is proportional to the deviation of the particle density from the integer filling; the constant A is explicitly given in Appendix A. Thus the stationary solutions correspond to the commensurate transition. In the noncommensurate regime there is no phase transition, but one can still use Eq. (11) if the deviation from the integer filling is small.

1. Commensurate case

Let us analyze the fate of the current-carrying case if the mean number of bosons per site is integer. Equation (11) supports stationary states of the form

$$\psi(x, \mathbf{z}) = \sqrt{r - p^2} e^{ipx}, \tag{13}$$

where $\mathbf{z}$ denotes the $d-1$-dimensional space of transverse coordinates. Without any further analysis it is obvious that current states become unstable at $p \gtrsim \sqrt{r} \sim 1/\xi$, i.e., the critical momentum vanishes at the superfluid-insulator transition point. To be more precise, we can evaluate the spectrum of small fluctuations of Eq. (11) around the stationary solution (13):

$$\omega^2(\mathbf{q}) = r - p^2 + \mathbf{q}^2 \pm \sqrt{(r-p^2)^2 + 4p^2 q_x^2 \xi^4}, \tag{14}$$

where q is the wave vector characterizing the fluctuations around the state (13). In the long-wavelength limit $|\mathbf{q}| \to 0$ the expression above yields simplified frequencies for the amplitude and the phase modes:

$$\omega_1^2(\mathbf{q}) \approx 2(r-p^2) + \frac{r+p^2}{r-p^2} q_x^2 + \mathbf{q}_\perp^2, \tag{15}$$

$$\omega_2^2(\mathbf{q}) \approx q_x^2 \frac{r-3p^2}{r-p^2} + \mathbf{q}_\perp^2. \tag{16}$$

The first (amplitude) branch is always gapped unless $p^2 > r$ and therefore is stable against small fluctuations. On the contrary, the second, phase mode, becomes unstable at $p > p_c = \sqrt{r/3}$. We would like to stress that the relativistic nature of excitations is crucial to get this instability. Despite being continuum Eq. (11) relies on the presence of the underlying lattice, which breaks the translational invariance. Otherwise the equations of motion would be Gallilean invariant and no critical current would exist.

From the analysis above we see that close to the superfluid-insulator phase transition current states become unstable at momenta inversely proportional to the correlation length of the condensate. As one goes deeper into the superfluid regime the correlation length decreases saturating at 1 (in the lattice units) and we come back to the Gross-Pitaveskii result of instability occurring at $p = \pi/2 \sim 1$.

2. Incommensurate case

It is also interesting to consider the stability of the current states at the noncommensurate filling. In this case the system remains superfluid at arbitrarily strong interactions [25]. If

the interactions are weak the system is in the Gross-Pitaveskii regime and the filling is not important. In this case we expect a usual modulational instability at $p \approx \pi/2$. At the same time, when the interaction strength becomes very large, we can think about excess particles as hard-core bosons moving on top of the Mott insulator. But in turn, this would be equivalent to a spin-one-half system. At the mean-field level we can use again spin-wave theory to see that p_c is exactly equal to $\pi/2$. This suggests that p_c should have a minimum at the intermediate interaction strength.

The solution of Eq. (11) corresponding to the noncommensurate filling factor can be written as

$$\psi(x,\mathbf{z},t) = \rho\, e^{ipx+i\mu t}, \tag{17}$$

where $\rho=\sqrt{r+\mu^2-p^2}$ and μ is related to the deviation from integer filling δn:

$$\delta n = A\mu\rho^2. \tag{18}$$

As in the commensurate case, in the long-wavelength limit there are two branches describing a gapped amplitude mode and gapless phase fluctuations. The dispersion of the latter for $\mathbf{q}$ parallel to the x axis reads

$$\omega(q) = \frac{2\mu p}{2\mu^2+\rho^2}q + \frac{\rho}{2\mu^2+\rho^2}\sqrt{3\rho^2-2r}|q|. \tag{19}$$

From this we observe that the current state first becomes unstable when $3\rho^2=2r$. Together with Eq. (18) this gives the critical momentum

$$p_c = \sqrt{\frac{r}{3}+\frac{9}{4r^2}\frac{\delta n^2}{A^2}}. \tag{20}$$

This result reduces to the commensurate limit for $\delta n=0$. However, for any nonzero δn it shows that p_c reaches the minimum value $p_c^{\bigstar} \propto \delta n^{1/3}$ at $r_0 \propto \delta n^{2/3}$ and then diverges as $r\to 0$. While the divergence is the spurious result of the continuum approximation; it should be cut off by the lattice at $p\approx 1$, the existence of the minimum agrees with the simple general argument given above.

C. Gutzwiller approximation

Having derived the conditions for the stability of the current-carrying condensate in a lattice in the two extreme limits, one can try to find a unifying approach, which interpolates between them. A natural choice is the Gutzwiller approximation. This is a time-dependent generalization of the standard mean-field theory, where the wave function is assumed to be factorizable:

$$|G\rangle = \prod_j \left[\sum_{n=0}^{\infty} f_{jn}|n\rangle_j\right]. \tag{21}$$

Here j denotes a site index and n site occupation. The ansatz (21) supplemented by self-consistency conditions leads to equations of motion:

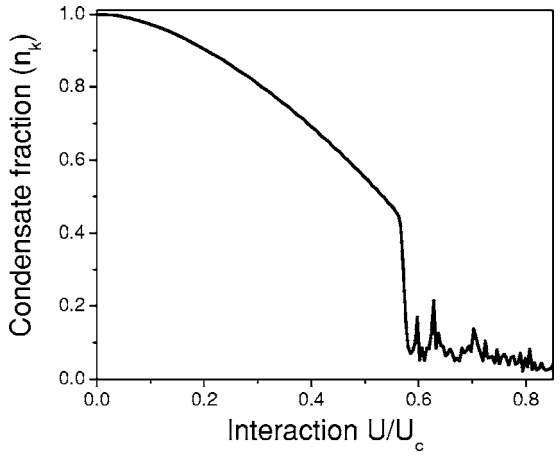

FIG. 3. Condensate fraction as a function of scaled interaction for a two-dimensional condensate with filling $N=1$ evaluated within Gutzwiller approximation on a square lattice of size 80×2 [40]. The initial momentum is $p=\pi/5$. The other parameters are $J=1$ (so that the interaction strength corresponding to the transition to the Mott state is $U_c\approx 23.2$) and the interaction increases in time as $U=0.04t$. The condensate motion clearly becomes unstable at certain interaction ($U/U_c\approx 0.57$), which marks the dynamical transition.

$$-i\dot{f}_{jn} = \frac{U}{2}n(n-1)f_{jn} - Jz(\sqrt{n}f_{j,n-1}\psi_j + \sqrt{n+1}f_{j,n+1}\psi_j^*), \tag{22}$$

where

$$\psi_j \equiv \frac{1}{z}\sum_{i\in O}\langle G|a_i|G\rangle. \tag{23}$$

O is the set of nearest neighbors to j and z is the coordination number ($z=2d$ for a hypercubic lattice). In practice the sum in Eq. (21) is limited to a finite number of states, on each site, so that only a finite number of equations need to be solved. We checked that in our numerical simulations we take sufficient number of states so that the results are insensitive to the truncation. In particular, for $N=1$ we compared simulations for the spectrum truncated at five and ten states per site and the results were practically indistinguishable. The Gutzwiller approximation can be justified at high dimensions, where the coordination number z becomes large. In this sense it is reminiscent to the dynamical mean-field theory [39]. In reality, it is necessary to calculate first quantum corrections to the evolution governed by Eq. (22) to see the validity of the Gutzwiller result at a given dimensionality. We will postpone such an analysis until the next section.

To find numerically the position of the dynamical instability corresponding to Eq. (22) we can carry out one of the following procedures. (i) Starting from the noninteracting state ($U=0$), where the Gutzwiller ansatz becomes exact, and a given phase gradient p we adiabatically increase U. Observing either the current or the condensate fraction (which we define as the population of the state with the momentum p) we can identify the critical interaction at which the motion becomes unstable (see Fig. 3). (ii) Alternatively we can find numerically the mean-field ground state corresponding to

given U and J and adiabatically increase a gauge potential so that Eq. (23) modifies to

$$\psi_{j,\mathbf{l}} \equiv \frac{1}{z}\left(\langle G|a_{j+1,\mathbf{l}}|G\rangle e^{i\phi(t)} + \langle G|a_{j-1,\mathbf{l}}|G\rangle e^{-i\phi(t)} + \sum_{\mathbf{l}' \in O'} \langle G|a_{j,\mathbf{l}'}|G\rangle\right). \quad (24)$$

Here we explicitly introduced indices along the current j and in the transverse direction $\mathbf{l}$; O' is a subset of O, which excludes the sites $\{j\pm1,\mathbf{l}\}$. If the system is stable then the condensate remains at the momentum $p=0$ in a moving lattice, which is of course equivalent to a moving condensate with $p=\phi(t)$ in a stationary lattice. Once the motion becomes unstable the distribution at $p=0$ rapidly drops. The second approach is favorable, because it does not require quantization of the momentum in units of $2\pi/M$ in finite systems of longitudinal size M, where the actual calculations are performed.

Identifying the point of dynamical instability as described above for different interaction strengths we can construct a mean-field phase diagram separating stable and unstable condensate motion for both integer and noninteger filling factors (see Fig. 4). This phase diagram is in complete agreement with what we expected from the analysis given in the previous subsections. Thus at small interactions the critical momentum approaches $\pi/2$ for any filling or dimensionality of the lattice. At integer filling the critical momentum vanishes at the point of commensurate superfluid-insulator transition. In the incommensurate case the critical momentum first goes down with the interaction strength and then increases back to $\pi/2$ in the strongly interacting regime.

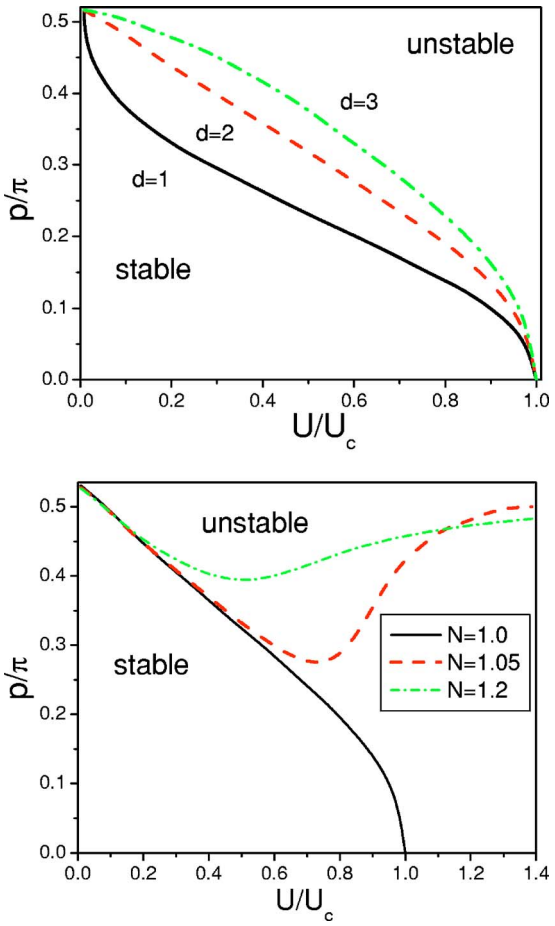

FIG. 4. Mean-field phase diagram separating stable and unstable motion of condensate. The vertical axis is the condensate momentum in the inverse lattice units and the horizontal axis is the normalized interaction. The top graph shows the result for integer filling $N=1$ at different spatial dimensions. The bottom graph describes a two-dimensional lattice with different filling factors.

IV. BEYOND MEAN-FIELD THEORY. CURRENT DECAY DUE TO FLUCTUATIONS

The analysis given in the previous section is valid only at the mean-field level. Quantum and thermal fluctuations can destroy the current by either phase-slip tunneling or thermal activation. The main goal of this section is to derive leading contributions to the decay rate and check the validity of the mean-field results. To simplify the analysis we will concentrate on the two tractable limits: the Gross-Pitaveskii regime describing the system deep in the superfluid phase and the Ginzburg-Landau regime, which is valid in the vicinity of the superfluid insulator transition, where the correlation length becomes large compared to the lattice constant. Also for simplicity we assume that the filling is large and integer so that one can use the quantum-rotor model.

A. Gross-Pitaveskii regime

1. Current decay due to quantum tunneling

As we argued above, the current state with $p<\pi/2$ is stable with respect to small fluctuations. However, this state does not correspond to the energy minimum, which has no current. So we conclude that such a state must be metastable. Contrary to a uniform system, where the momentum can be gauged away via the Gallilean transformation, in a lattice there is a preferred reference frame. This immediately implies that such a metastable state should be able to spontaneously decay because of quantum tunneling.

In the leading order in U/JN, which plays the role of the effective Planck's constant for this problem [41], the tunneling rate (Γ) corresponds to the action (S) of the bounce solution (instanton) of the classical equations of motion in the inverted potential [42]:

$$\Gamma \propto e^{-S}. \quad (25)$$

We will not attempt to compute the prefactor here and will concentrate only on S. We just point out that the prefactor scales with the system size and in the thermodynamic limit the tunneling rate per unit volume is size independent. Explicitly the action reads as

$$S=\sum_{j,\mathbf{l}}\int d\tau\left[\frac{1}{2U}\left(\frac{d\phi_{j,\mathbf{l}}}{d\tau}\right)^2-2JN\cos(\phi_{j,\mathbf{l}+\mathbf{1}}-\phi_{j,\mathbf{l}})-2JN\cos(p+\phi_{j+1,\mathbf{l}}-\phi_{j,\mathbf{l}})\right],\tag{26}$$

where as before j denotes the coordinate along the current direction and $\mathbf{l}$ corresponds to the transverse coordinates. In Eq. (26) we redefined phases compared to Eq. (10): $\phi_j \to \phi_j - px_j$ so that $\phi_j=0$ corresponds to a metastable current state and the new phases are the fluctuations around this state. It is convenient to redefine the imaginary time τ, measuring it in Josephson time units: $\tau \to \tau/\sqrt{UNJ}$. Then it is easy to see that

$$S=\sqrt{\frac{JN}{U}}s,\tag{27}$$

where

$$s=\sum_{j,\mathbf{l}}\int d\tau\left[\frac{1}{2}\left(\frac{d\phi_{j,\mathbf{l}}}{d\tau}\right)^2-2\cos(\phi_{j,\mathbf{l}+\mathbf{1}}-\phi_{j,\mathbf{l}})-2\cos(p+\phi_{j+1,\mathbf{l}}-\phi_{j,\mathbf{l}})\right].\tag{28}$$

The desired instanton trajectory is the solution of the Euler-Lagrange equations, which can be obtained extremizing the action with respect to the phases $\phi_{j,\mathbf{l}}$ and subject to a boundary conditions $\phi_{j,\mathbf{l}}=0$ at $\tau=\pm\infty$ and at $|\mathbf{l}|,|j|=\infty$.

Before proceeding with a general analysis in higher spatial dimensions let us consider the case $d=1$ first. In this work we are interested in the decay close to the critical current $p_c=\pi/2$. Clearly as $p\to p_c$ the effective tunneling barrier becomes weaker and weaker and hence we can expand Eq. (28) in powers of ϕ_j:

$$s\approx\sum_j\int d\tau\left[\frac{1}{2}\left(\frac{d\phi_j}{d\tau}\right)^2+\cos(p)(\phi_{j+1}-\phi_j)^2-\frac{(\phi_{j+1}-\phi_j)^3}{3}\right].\tag{29}$$

This expansion is similar to that used in the analysis of thermally mediated decomposition near the spinodal point [43]. In the action above we used that $\sin p\approx\sin p_c=1$. Now we can do another rescaling:

$$\phi_j=\cos(p)\tilde{\phi}_j,\quad \tau=\frac{\tilde{\tau}}{\sqrt{\cos(p)}},\tag{30}$$

which simplifies the action even further:

$$s\approx(\cos p)^{5/2}\tilde{s},\tag{31}$$

where

$$\tilde{s}=\sum_j\int d\tilde{\tau}\,\frac{1}{2}\left(\frac{d\tilde{\phi}_j}{d\tilde{\tau}}\right)^2+(\tilde{\phi}_{j+1}-\tilde{\phi}_j)^2-\frac{(\tilde{\phi}_{j+1}-\tilde{\phi}_j)^3}{3}.\tag{32}$$

Note that $\tilde{s}$ is just a number of the order of 1 so that Eq. (31) completely determines the momentum dependence of the action. The scaling (30) guarantees that the original phases ϕ_j remain small for the instanton trajectory and Eq. (29) is indeed a correct asymptotical form of Eq. (28).

Since the action $\tilde{s}$ contains no small parameters, the bounce solution should be localized within a few sites. Without loss of generality we can assume that the maximum phase difference develops between the sites labeled by $j=0$ and $j=1$. For the rest of the system the phase gradients are relatively small so we can neglect cubic terms. Then those degrees of freedom can be integrated out:

$$\tilde{\phi}_j(\tau)=\pm\int\frac{d\omega}{4\pi}\alpha(\omega)e^{-i\omega\tau}\lambda(\omega)^{j-1},\tag{33}$$

where $\alpha(\tau)=\tilde{\phi}_1(\tau)-\tilde{\phi}_0(\tau)$ and $\alpha(\omega)$ is its Fourier transform;

$$\lambda(\omega)=1+\frac{\omega^2}{4}-\frac{\omega}{\sqrt{2}}\sqrt{1+\frac{\omega^2}{8}}.\tag{34}$$

Substituting Eq. (33) into Eq. (32) we find

$$\tilde{s}\approx\int d\tau\left[\frac{1}{4}\left(\frac{d\alpha(\tau)}{d\tau}\right)^2+\alpha^2(\tau)-\frac{1}{3}\alpha^3(\tau)\right]+\int\frac{d\omega}{4\pi}|\alpha(\omega)|^2\frac{|\omega|}{|\omega|+\sqrt{8+\omega^2}}.\tag{35}$$

Clearly, if we ignore the last term in the expression (35) we get the action of a single particle moving in a metastable potential. The last term represents a dissipativelike contribution coming from the rest of the chain. If we ignore this term then the solution extremizing Eq. (35) is

$$\alpha(\tau)=\frac{3}{\cosh^2 t/\sqrt{2}}.\tag{36}$$

This yields $\tilde{s}=24/5\equiv 4.8$. In a general case with dissipation we can try a variational ansatz solution:

$$\tilde{\alpha}(\tau)=\frac{A}{\cosh^2 r\tau}.\tag{37}$$

A simple numerical analysis gives

$$r\approx 0.64,\quad A\approx 3.31,\quad \tilde{s}\approx 7.11.\tag{38}$$

So the action is about a factor of 1.5 larger than without the bath degrees of freedom. Using Eqs. (33) and (38) one can verify the consistency of the harmonic approximation used for the sites other than "1" and "0." In particular, it is straightforward to get

$$\frac{|\tilde{\phi}_2(0)-\tilde{\phi}_1(0)|}{\alpha(0)} \approx 0.326, \tag{39}$$

which is relatively small. The difference between phases in further nearest-neighbor sites is even less. Therefore for them the harmonic approximation is justified even better.

Instead of harmonic treatment of the phases other than $\tilde{\phi}_1$ and $\tilde{\phi}_2$ we can exactly take into account the four nearest-neighbor sites and ignore the rest of the chain. Then the instanton solution is parametrized by the two independent angles α and β:

$$\tilde{\phi}_0 = -\tilde{\phi}_{-1} = \alpha/2, \quad \tilde{\phi}_1 = -\tilde{\phi}_{-2} = \alpha/2 + \beta. \tag{40}$$

Substituting this into the action and solving the corresponding Euler-Lagrange equations one can show that in this case $\tilde{s} \approx 6.1$, which is about a factor of 1.26 larger than the result with $\beta \equiv 0$. This number is the exact lower bound for the action $\tilde{s}$ since the other degrees of freedom can only increase the action. We will not further attempt to improve the accuracy of $\tilde{s}$ noting only that the variational result $\tilde{s} \approx 7.1$ should be very close to the exact value.

We can straightforwardly generalize the one-dimensional results to higher spatial dimensions. In particular, using the same arguments as before close to the critical current we can expand the action (28) up to the cubic order in $\phi_{j,\mathbf{l}}$:

$$s \approx \sum_{j,\mathbf{l}} \int d\tau \left[\frac{1}{2}\left(\frac{d\phi_{j_\mathbf{l}}}{d\tau}\right)^2 + \cos(p)(\phi_{j+1,\mathbf{l}} - \phi_{j,\mathbf{l}})^2 + \sum_{\mathbf{l}' \in \mathbf{O}'} (\phi_{j,\mathbf{l}'} - \phi_{j,\mathbf{l}})^2 - \frac{1}{3}(\phi_{j+1,\mathbf{l}} - \phi_{j,\mathbf{l}})^3 \right]. \tag{41}$$

Note that at $p \to \pi/2$ only longitudinal modes become soft, acquiring a prefactor $\cos p$ in front of the quadratic term in the action. This implies that the transverse width of the instanton should be much larger than its longitudinal size and we can safely use the continuum approximation for the phases along the transverse directions. Then instead of Eq. (41) we derive

$$s \approx \sum_j \int d\tau d^{d-1}x \left[\frac{1}{2}\left(\frac{d\phi_j}{d\tau}\right)^2 + \left(\frac{d\phi_j}{d\mathbf{x}}\right)^2 + \cos(p)(\phi_{j+1} - \phi_j)^2 - \frac{1}{3}(\phi_{j+1} - \phi_j)^3 \right]. \tag{42}$$

In this equation $\mathbf{x}$ denotes transverse coordinates which reside in a $d-1$-dimensional space. As in the one-dimensional case we can rescale

$$\phi = \cos(p)\tilde{\phi}, \quad \tau = \frac{\tilde{\tau}}{\sqrt{\cos(p)}}, \quad x = \frac{\tilde{x}\sqrt{2}}{\sqrt{\cos p}}. \tag{43}$$

In this way the action (42) becomes

$$s \approx (p_c - p)^{(6-d)/2}\tilde{s}_d, \tag{44}$$

where

$$\tilde{s}_d = 2^{(d-1)/2} \sum_j \int d^d\zeta \left[\frac{1}{2}\left(\frac{d\tilde{\phi}_j}{d\boldsymbol{\zeta}}\right)^2 + (\tilde{\phi}_j - \tilde{\phi}_{j+1})^2 - \frac{1}{3}(\tilde{\phi}_j - \tilde{\phi}_{j+1})^3 \right]. \tag{45}$$

Here $\boldsymbol{\zeta} = (\tilde{\tau}, \tilde{\mathbf{x}})$ is a d-dimensional space-time coordinate. As before $\tilde{s}_d$ is just a number, which depends only on dimensionality. The result (44) is quite remarkable. First of all it shows that the action in higher dimensions vanishes much more slowly near the critical current. From the scaling (43) it is obvious that the characteristic transverse dimension of the instanton scales as $1/\sqrt{p_c - p} \gg 1$, justifying the continuum approximation. Above $d=6$ the tunneling action would experience a discontinuous jump at $p=p_c$, however, since we deal with $d \leqslant 3$ this is not relevant. Now let us try to estimate $\tilde{s}_d$. We again proceed in the same spirit as in the one-dimensional case. In the first approximation we consider only a single phase slip $\tilde{\phi}_1 = \alpha/2$, $\tilde{\phi}_2 = -\alpha/2$ and treat the motion of other phases in the harmonic approximation. The corresponding dimensionless action reads

$$\tilde{s}_d = 2^{(d-1)/2} \int d^d\zeta \left[\frac{1}{4}(\boldsymbol{\nabla}\alpha)^2 + \alpha^2 - \frac{1}{3}\alpha^3 \right] + \frac{1}{2}\int \frac{d^dk}{(2\pi)^d} |\alpha(\mathbf{k})|^2 \frac{k}{k + \sqrt{8 + k^2}}, \tag{46}$$

where $\alpha(\mathbf{k})$ is the Fourier image of $\alpha(\mathbf{x})$. If we ignore the last dissipative term in Eq. (46), then our action is identical to that considered in Ref. [42] for the decay of a false vacuum. In that work it was argued that the bounce solution is spherically symmetric and it satisfies the following equations of motion:

$$\frac{1}{2}\frac{1}{\zeta^d}\frac{d}{d\zeta}\left(\zeta^d \frac{d\alpha}{d\zeta}\right) = 2\alpha - \alpha^2, \tag{47}$$

with the boundary conditions $\alpha(\infty)=0$ and $\alpha'(0)=0$. These equations can be easily solved numerically and the result is

$$\tilde{s}_2 \approx 21.92, \quad \tilde{s}_3 \approx 87.32. \tag{48}$$

So it is clear that at higher dimensions not only the exponent of $(p_c - p)$ in the instanton action gets lower but also the numerical prefactor gets larger. Now we can find the correction to the action due to the bath degrees of freedom coming from the last term in Eq. (46). Instead of using the variational approach as we did in the one-dimensional case, we will use the exact solution of Eq. (47) to evaluate the contribution of the bath term in the action. This will be the *exact* upper bound of the action $\tilde{s}_d$. Direct evaluation of Eq. (46) gives

$$4.8 < \tilde{s}_1 < 8.0, \quad 21.9 < \tilde{s}_2 < 27.6, \quad 87.3 < \tilde{s}_3 < 97.5. \tag{49}$$

Obviously the local approximation $\phi_j = 0$ for $j \neq 0, 1$ works better and better at higher dimensions implying that the effective size of the instanton in the longitudinal direction (along the current) decreases with the dimensionality of the space.

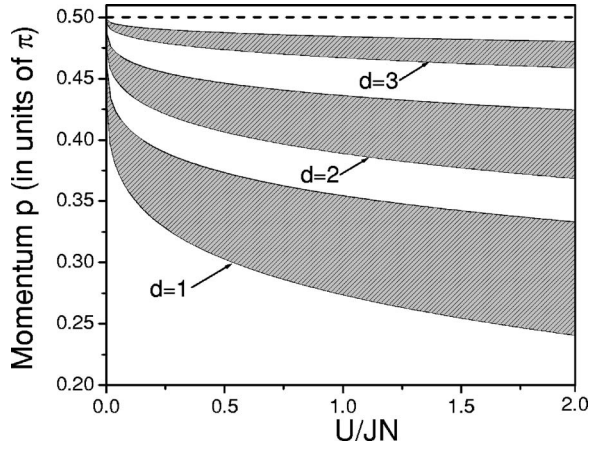

FIG. 5. Large N zero-temperature phase diagram for the nonequilibrium superfluid-insulator transition. The dashed line represents mean-field transition at $p=\pi/2$. The shaded regions correspond to the tunneling action satisfying $1\leqslant S\leqslant 3$, obtained within the discrete phase model in different spatial dimensions. Below the shaded regions the tunneling action is large and the current decay is slow, so the superfluid state is stable for long time scales. Above the shaded regions the current decays very fast and the superfluid state is unstable.

Because the decay rate is strongly (exponentially) dependent on momentum and coupling constants we can approximately define the stable phase at which the tunneling action is larger than some number, say $S>3$, and unstable phase, when there is no exponential suppression of the tunneling of phase slips, say $S<1$. The region in between will denote the crossover between the stable and unstable regimes. In this way we can define a crossover phase diagram (Fig. 5). We see that except for $U/JN\ll 1$, there is a very strong broadening of the classical transition in one dimension. On the contrary, in the three-dimensional case effects of quantum fluctuations are relatively weak and the crossover is very sharp. We would like to point out that the derivation given here is valid only deep in the superfluid regime $U/JN\ll 8d$. Close to the critical point it is necessary to use the coarse-grained description which we discuss later.

To summarize this subsection we write explicit expressions for the tunneling action in the phase model in three spatial dimensions:

$$S_{d=1}\approx 7.1\sqrt{\frac{JN}{U}}\left(\frac{\pi}{2}-p\right)^{5/2}, \tag{50}$$

$$S_{d=2}\approx 25\sqrt{\frac{JN}{U}}\left(\frac{\pi}{2}-p\right)^{2}, \tag{51}$$

$$S_{d=3}\approx 93\sqrt{\frac{JN}{U}}\left(\frac{\pi}{2}-p\right)^{3/2}. \tag{52}$$

2. Thermally activated current decay

Now let us turn our attention to broadening of the mean-field transition due to thermal fluctuations. A general formalism for finding the decay rate was developed by Langer [44]. It was later successfully applied to quasi-one-dimensional superconductors [30,31] and to three-dimensional superfluids at small currents [45].

Before proceeding with this general method let us point out an essential difference between conventional condensed-matter systems and the cold atoms systems addressed in this work. In the former, it is the environment which introduces thermal noise and dissipation [46] to the system leading to diffusion in energy space and eventually thermal activation. In cold atom systems, by contrast, the temperature is introduced into the system during the preparation of the condensate, i.e., the initial state of the condensate is described by a thermal density matrix rather than a pure wave function. Later the system is essentially isolated from the environment and evolves according to the Hamiltonian equations of motion. We point out that the formalism of Ref. [44] was based on very general assumptions, and therefore should be independent of the details of the thermal fluctuations. Nevertheless, certain issues arise that require special attention. Consider, for example, a superfluid flowing in a container whose walls act as the thermal bath. The wall as well as the thermal fluctuations arising from it set a preferred reference frame, breaking the Galilean invariance of the superfluid and thus allowing for the current decay. An isolated superfluid, on the other hand, even if prepared at finite temperature, is Galilean invariant. Thus current in such a superfluid cannot decay unless there is an external potential, such as a lattice, that sets a preferred reference frame. Because we are interested in the current decay in the limit where the lattice is strong and boson Hubbard model (BHM) is applicable, this subtlety is irrelevant for our consequent analysis. The effect of breaking Galilean invariance by weak external potential on thermally activated current decay in one-dimensional superconductors was recently studied in Ref. [47].

To simplify the analysis we assume that the temperature is small so that there is no difference between the energy and the free energy. Indeed, the difference between the two amounts to the product $T\mathcal{S}$, where $\mathcal{S}$ is the entropy of the system. At small temperatures the latter vanishes in the superfluid as T^d so that the product $T\mathcal{S}$ goes to zero at least as T^2 at $T\to 0$ and is always negligible compared to the activation energy, which does not depend on temperature.

As in the previous subsection, we first consider the one-dimensional case. Following Refs. [31,44] we find the stationary solutions of the classical equations of motion:

$$\frac{1}{2}\frac{d^2\phi_j}{d\tau^2}=\sin(p+\phi_{j+1}-\phi_j)+\sin(-p+\phi_{j-1}-\phi_j). \tag{53}$$

Clearly $\phi_j=0$ describes a metastable state carrying the current $2JN\sin p$. We note again that phases in Eq. (53) are the deviations from the metastable current state. The other saddle-point solution separating the states with different currents is

$$\phi_j=\begin{cases}(p'_{\pm}-p)j & j<0\\ \pi+p'_{\pm}(j-2)-pj & j\geqslant 1,\end{cases} \tag{54}$$

where $p'_{-}\approx p-(\pi-2p)/M$ and $p'_{+}\approx p+(\pi+2p)/M$ for a periodic chain of size M. The indices "–" and "+" correspond

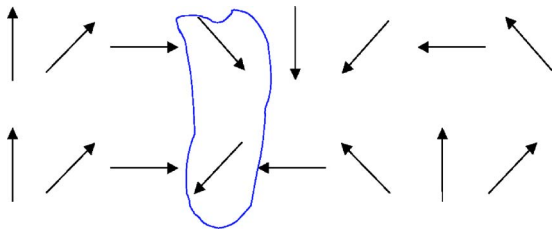

FIG. 6. Schematic representation of a metastable current carrying state and an unstable saddle-point solution. The arrows represent the superfluid phase at different sites of the lattice.

to phase slip and antiphase slip, respectively, with the convention that the slip reduces the current. Schematically the saddle-point and the metastable solutions are depicted in Fig. 6. Clearly the energy difference between the two states is

$$\Delta E_- = 2JN[2\cos p - \sin p(\pi - 2p)] \tag{55}$$

and

$$\Delta E_+ = 2JN[2\cos p + \sin p(\pi + 2p)]. \tag{56}$$

Correspondingly, the decay rate to lower (higher) current state is proportional to

$$\Gamma_{\mp} \propto e^{-\beta \Delta E_{\mp}} = e^{-2JN\beta[2\cos p \mp (\pi \mp 2p)\sin p]}. \tag{57}$$

In particular when $p \to \pi/2$ we have

$$\Gamma_- \propto e^{-(4/3)NJ\beta(\pi/2-p)^3}. \tag{58}$$

In the one-dimensional case it is also straightforward to evaluate the prefactor in the decay rate. We give details of such derivation in Appendix B and quote only the final result here:

$$\Gamma_- \approx \frac{64\cos p}{\pi\tau}\sqrt{\frac{JN}{U}}\exp\left(-\frac{\pi/2-p}{4}\tan p - \frac{4NJ}{T}[\cos p - (\pi/2-p)\sin p]\right), \tag{59}$$

$$\Gamma_+ \approx \frac{64\cos p}{\pi\tau}\sqrt{\frac{JN}{U}}\exp\left(\frac{\pi/2+p}{4}\tan p - \frac{4NJ}{T}[\cos p + (\pi/2+p)\sin p]\right). \tag{60}$$

Here τ is a relaxation time of the condensate towards thermal equilibrium, which we will leave as a phenomenological parameter.

We can now compare the leading exponential terms for the two current decay mechanisms. Thus if we require that the exponent in Eq. (57) is equal to the tunneling action computed in the previous section we can find when the two exponents coincide. It is convenient to introduce a characteristic temperature scale T_Q, at which the energy of the zero-point fluctuations is equal to the thermal energy of the corresponding classical system. Using Bogoliubov's approximation one finds that

$$T_Q = \frac{2\sqrt{2}}{\pi}\sqrt{NJU}. \tag{61}$$

We can now rewrite the expression for Γ_- at p close to $p_c = \pi/2$ in a more convenient form:

$$\Gamma_- \approx \frac{64\cos p}{e^{1/4}\pi\tau}\sqrt{\frac{JN}{U}}\exp\left[-\frac{\sqrt{2}\pi}{3}\sqrt{\frac{NJ}{U}}\frac{T_Q}{T}(p_c-p)^3\right]. \tag{62}$$

Note that the exponent in the expression above coincides with that in Eq. (50) when

$$T^\star \approx 0.21\, T_Q\sqrt{\pi/2-p}. \tag{63}$$

The temperature $T^\star$ separates regimes of thermally activated and quantum current decay. Thus if $T<T^\star$ thermal phase slips are unimportant so that quantum tunneling dominates the decay and vice versa. Note that unless p is very close to $\pi/2$, the crossover temperature $T^\star$ is of the order of the characteristic Josephson energy T_Q (or equivalently the sound velocity in the lattice units). Under present experimental conditions it is very easy to achieve $T \ll T_Q$ and thus $T<T^\star$ and therefore to observe current damping due to quantum phase slips.

In higher dimensions we cannot find an explicit analytic expression for the energy of the metastable state. However, we can get an approximate result near the critical current. Using again the idea that the transverse fluctuations can be treated in the continuum approximation and expanding $\cos(p+\phi_{j+1}-\phi_j)$ up to the third order in phases we can write the energy in the approximate form:

$$E_d \approx JN\sum_j \int d^{d-1}x\left[\left(\frac{d\phi_j}{dx}\right)^2 + \cos(p)(\phi_{j+1}-\phi_j)^2 - \frac{1}{3}(\phi_{j+1}-\phi_j)^3\right], \tag{64}$$

where $\phi_j(x)$ is the nontrivial solution of the corresponding Euler-Lagrange equations vanishing at $x\to\infty$. After rescaling $\phi = \cos(p)\tilde{\phi}$ and $x = \tilde{x}\sqrt{2}/\sqrt{\cos p}$ we find

$$E_d \approx JN\, 2^{(d-1)/2}(p_c-p)^{(7-d)/2}\sum_j \int d^{d-1}\tilde{x}\left[\frac{1}{2}\left(\frac{d\tilde{\phi}_j}{d\tilde{x}}\right)^2 + (\tilde{\phi}_{j+1}-\tilde{\phi}_j)^2 - \frac{1}{3}(\tilde{\phi}_{j+1}-\tilde{\phi}_j)^3\right]. \tag{65}$$

Note that the integral in the expression above coincides with $\tilde{s}_{d-1}$ up to a number $2^{(d-2)/2}$. So using results (50) and (51), and (58) we immediately conclude that

$$E_1 \approx 1.3\, JN\left(\frac{\pi}{2}-p\right)^3, \tag{66}$$

$$E_2 \approx 10\, JN\left(\frac{\pi}{2}-p\right)^{5/2}, \tag{67}$$

$$E_3 \approx 35JN\left(\frac{\pi}{2}-p\right)^2. \tag{68}$$

Correspondingly, the exponents in the thermal and quantum decay rates become the same at a temperature

$$T^\star \approx 0.44\, T_Q\sqrt{\pi/2-p} \tag{69}$$

both in two and three dimensions. This crossover temperature is about a factor of 2 higher than in the one-dimensional case (63). If p is not too close to $\pi/2$, $T^\star$ is again of the order of T_Q and thus the quantum tunneling should be responsible for the current damping below the mean-field transition at experimentally relevant temperatures.

B. Current decay in the vicinity of the SF-MI phase transition

As we show in Appendix A the quantum action in imaginary time takes the following form:

$$S = C\int d^dz dx\left|\frac{d\psi}{d\mathbf{z}}\right|^2+\left|\frac{d\psi}{dx}\right|^2-|\psi|^2+\frac{1}{2}|\psi|^4. \tag{70}$$

Here z denotes the imaginary time and transverse coordinates which form a d-dimensional space, x is a longitudinal coordinate along the current. Note that in this section we measure coordinates in units of the coherence length. This is because we focus on the commensurate case and hence we are interested only in the superfluid regime $r>0$ [see Eq. (11)]. In this case it is convenient to rescale $x\to x/\sqrt{r}$ to simplify the notations (in the original lattice units x is measured in the units of the correlation length ξ). The constant C depends on the original microscopic parameters of the underlying Hamiltonian. Within the variational ansatz described in Appendix A we find [38]

$$C = \frac{1}{u}\frac{1}{2(2d)^{d/2}}(1-u)^{(3-d/2)}, \tag{71}$$

where $u=U/8dJN$ is the dimensionless interaction;

$$\xi = \frac{1}{\sqrt{2d(1-u)}}. \tag{72}$$

In the case when thermal fluctuations are more important than the zero-point motion, we are interested in the energy functional rather than the action:

$$\mathcal{E} = C'\int d^{d-1}z dx\left|\frac{d\psi}{d\mathbf{z}}\right|^2+\left|\frac{d\psi}{dx}\right|^2-|\psi|^2+\frac{1}{2}|\psi|^4, \tag{73}$$

where $\mathbf{z}$ comprises now $d-1$ transverse coordinates only. The value of the constant C' can be found within the mean-field approximation (see Appendix A):

$$C' = JN\frac{1}{u(2d)^{d/2-1}}(1-u)^{2-d/2}. \tag{74}$$

Before proceeding we would like to point out that the mean-field expressions for ξ and C are valid in the vicinity of the quantum phase transition at large spatial dimensions. For example, at $d=1$ the superfluid-insulator transition belongs to the Kosterlitz-Thouless universality class and it is characterized by proliferation of vortices [48,49]. In particular, dissipation in two spatial dimensions in the vicinity of the thermal superfluid-to-normal fluid transition, which is also of the Kosterlitz-Thouless class was studied in Ref. [50]. It was shown that the dissipation comes from unbinding of existing vortices and it does not have an exponential suppression. So while the mean-field description near the quantum critical point in one dimension is questionable, we believe that it is justified in two and especially in three spatial dimensions.

Decay of superconducting current in the GL model was studied by several authors. In particular, the exponent characterizing the decay rate in the one-dimensional case was studied in Ref. [30] and the prefactor setting the time scale was later found in Ref. [31]. In three dimensions at small currents the corresponding exponent was derived by Langer and Fisher [45], where it was shown that the decay rate vanishes as $\exp(-C/p)$ as $p\to 0$. However, here we are interested in quite the opposite limit $p\to p_c$, where the method used in that paper does not work.

Let us start our analysis from the quantum decay. We first emphasize that quantum in this context means due to fluctuations beyond the saddle-point approximation. Contrary to the Gross-Pitaveskii regime, where the classical description is well controlled by the smallness of the ratio U/JN, there is no obvious small parameter here. The validity of the mean-field description in this case can be checked *a posteriori* by explicit computation of quantum corrections. The other comment we would like to make is that the parameters C and ξ entering the Ginzburg-Landau action are generally renormalized and deviate from the mean-field results.

To compute the tunneling action we need to find a bounce solution of the classical equations of motion in imaginary time. Instead of using complex fields ψ_j we introduce two real fields η and ϕ describing amplitude and phase fluctuations around the metastable minimum:

$$\psi(x,\mathbf{z}) = \sqrt{1-k^2}[1+\eta(x,\mathbf{z})]e^{ikx+i\phi(x,\mathbf{z})}. \tag{75}$$

Here we intentionally use another notation k for the condensate momentum, because it is measured in the units of inverse correlation length ξ. It is related to the usual momentum p in inverse lattice units as $k=p\,\xi$. We can expect that close to the critical current both η and ϕ remain small and we can expand the action up to the cubic terms in these fields to find the correct asymptotical behavior of the instanton action at $k\to k_c$:

$$s \approx \frac{2}{3}\int d\mathbf{z}dx(\partial_{\mathbf{z}}\eta)^2+(\partial_{\mathbf{z}}\phi)^2+(\partial_x\eta)^2+(\partial_x\phi)^2+2(1-k^2)\eta^2$$
$$+4k\eta\partial_x\phi+2\eta(\partial_{\mathbf{z}}\phi)^2+2\eta(\partial_x\phi)^2+\frac{2}{\sqrt{3}}\eta^2\partial_x\phi+\frac{4}{3}\eta^3. \tag{76}$$

It is easier to start the analysis of Eq. (76) calculating the corresponding energy in $d=1$. This problem was already solved in Ref. [31] for all values of k. So we will use the asymptotic of their expression at $k\to k_c$ to compare with our result and thus check the validity of our scheme. It is easy to see that upon the transformation

$$\eta \to \eta - \frac{k}{1-k^2}\partial_x \phi \tag{77}$$

the cross term in η and ϕ vanishes in the quadratic part of Eq. (76). Since the amplitude η mode remains gapped at $k=k_c$ it can be disregarded and the approximate energy [which is equivalent to the action (76) at $d=0$] takes the form

$$\epsilon \approx \int dx \frac{1}{2}(\partial_x^2 \phi)^2 + 2\sqrt{3}(k_c-k)(\partial_x \phi)^2 - \frac{2}{\sqrt{3}}(\partial_x \phi)^3. \tag{78}$$

Upon rescaling

$$x \to \frac{x}{3^{1/4}2\sqrt{k_c-k}}, \quad \phi \to \phi \frac{3^{3/4}}{2}\sqrt{k_c-k} \tag{79}$$

we obtain

$$\epsilon \approx 93^{1/4}(k_c-k)^{5/2} \int dx (\partial_x^2 \phi)^2 + (\partial_x \phi)^2 - (\partial_x \phi)^3. \tag{80}$$

The last integral is just a number equal to the energy of the saddle point, which is a nontrivial solution of the Euler-Lagrange equations,

$$-2\frac{d^2\phi'}{dx^2} + 2\phi' - 3\phi'^{\,2} = 0, \tag{81}$$

where $\phi' \equiv d\phi/dx$. This equation has a simple solution:

$$\phi'(x) = \frac{1}{\cosh^2 x/2}, \tag{82}$$

which after substitution into Eq. (80) gives:

$$\epsilon \approx \frac{48}{5}3^{1/4}(k_c-k)^{5/2}. \tag{83}$$

This result coincides with that derived in Ref. [31] at $k \to k_c$. Now we can proceed with a general d-dimensional case. As in the previous section the instanton action in $d+1$ dimensions is equal to the barrier energy in d dimensions. After performing the transformations (77) and ignoring the gapped amplitude mode η we find

$$s \approx \int d^d z dx \frac{1}{2}(\partial_{\mathbf{z},x}^2 \phi)^2 + \frac{2}{3}(\partial_{\mathbf{z}} \phi)^2 + \frac{1}{2}(\partial_x^2 \phi)^2 + 2\sqrt{3}(k_c-k) \times (\partial_x \phi)^2 - \frac{2}{\sqrt{3}}(\partial_x \phi)^3. \tag{84}$$

It is easy to see that the rescaling required to make the action independent of the momentum is

$$x \to \frac{x}{3^{1/4}2\sqrt{k_c-k}}, \quad \phi \to \phi \frac{3^{3/4}}{2}\sqrt{k_c-k}, \quad z \to \frac{z}{6(k_c-k)}. \tag{85}$$

Upon these transformations the first term in the action becomes irrelevant and in the leading order in k_c-k the action reads

$$s_d = \frac{3^{(9-4d)/4}}{2^d}(k_c-k)^{(5-2d)/2} \int d\mathbf{z} dx (\boldsymbol{\nabla} \phi)^2 + (\partial_x^2 \phi)^2 - (\partial_x \phi)^3, \tag{86}$$

where $\boldsymbol{\nabla} = (\partial_{\mathbf{z}}, \partial_x)$ is the gradient in $d+1$ dimensions. For the classical energy, as we mentioned above, one has to substitute $d \to d-1$ in Eq. (86). The important difference between the result for the continuum model (86) and the lattice result (44) is that the power of the k_c-k in the prefactor in Eq. (86) is smaller than that in Eq. (44). Moreover, in $d=3$ the whole scaling breaks down suggesting the the instanton action becomes discontinuous at $d=3$ near the Mott transition.

We can evaluate the integral in Eq. (86) using the variational ansatz. For simplicity we will take a separable function

$$\phi(z,x) = A(z)\frac{\tanh \alpha x}{\cosh \beta x}, \tag{87}$$

where α and β are the variational parameters and the function $A(z)$ can be found solving the remaining one-dimensional problem. With this choice it is easy to show that in one and two dimensions we obtain

$$\alpha_{1d} \approx 0.32, \quad \beta_{1d} \approx 0.53, \quad s_{1d} \approx 73(k_c-k)^{3/2}, \tag{88}$$

$$\alpha_{2d} \approx 0.72, \quad \beta_{1d} \approx 1.08, \quad s_{2d} \approx 67(k_c-k)^{1/2}. \tag{89}$$

In three dimensions this variational ansatz gives $S_3 \to 0$, which implies breaking of the scaling as $k_c \to k$. Indeed, the power of (k_c-k) in Eq. (86) becomes negative. However, it is unphysical to expect any divergence near the point of instability. This indicates that the original ansatz that the longitudinal coordinate scales as $1/\sqrt{k_c-k}$ is not valid in this case and the tunneling action becomes momentum independent as $k \to k_c$. To see that this is indeed the case and to estimate the actual value of s in three dimensions we return to the the action (84) without preforming rescaling Eq. (85) and apply the variational ansatz (87). Then as $k \to k_c$ we find

$$\alpha_{3d} \approx 0.53, \quad \beta_{3d} \approx 0.8, \quad s_{3d} \approx 125. \tag{90}$$

Using the mean-field parameters C and ξ in Eq. (70) and the results (88)–(90) we can rewrite the tunneling action in the following form:

$$S_1 \approx \frac{5.7}{\xi^2}(1-\sqrt{3}p\,\xi)^{3/2}, \tag{91}$$

$$S_2 \approx \frac{3.2}{\xi}(1-\sqrt{3}p\,\xi)^{1/2}, \tag{92}$$

$$S_3 \approx 4.3. \tag{93}$$

The equilibrium superfluid-insulator phase transition corresponds to $\xi=\infty$. Notice that in one and two dimensions the tunneling action is always small as long as $\xi \gg 1$ and p is close to the critical momentum. This implies that at small currents the broadening of the nonequlibrium transition is very large. This is consistent with earlier numerical findings [22] and recent experiments [24]. In three dimensions, as we

argued above, the tunneling action is discontinuous at the transition, therefore the mean-field phase boundary is defined very well. So at $d=3$ at zero temperature we can accurately define a relatively sharp phase transition between the current carrying superfluid and the insulator.

Quite similar considerations apply to the current decay due to thermal fluctuations. The decay rate is determined by the ratio of the activation energy E_d and the temperature. In different spatial dimensions we get

$$E_1 \approx 1.3\frac{JN}{\xi^3}(1-\sqrt{3}p\,\xi)^{5/2}, \tag{94}$$

$$E_2 \approx 7.8\frac{JN}{\xi^2}(1-\sqrt{3}p\,\xi)^{3/2}, \tag{95}$$

$$E_3 \approx 8.6\frac{JN}{\xi}(1-\sqrt{3}p\,\xi)^{1/2}. \tag{96}$$

It is obvious that the thermal broadening is also strongest in one dimension. However, contrary to the quantum case, even at three dimensions close to the mean-field transition the activation barrier vanishes continuously. Only in four dimensions and above we would be able to define a sharp phase boundary separating current carrying superfluid and insulating phases at finite temperature.

We would like to point out that the thermal decay is strongly suppressed at low temperatures $T \ll JN/\xi$. Note that this condition is also necessary in order to observe the equilibrium superfluid-insulator transition and thus can be satisfied experimentally. Another important point is that the action for the quantum phase-slip tunneling in one and two dimensions is never large near the mean-field critical current. This implies that the quantum decay mechanism should be experimentally relevant at $d=1$ and $d=2$. This conclusion is similar to that reached in the previous section when we discussed current decay at small interactions.

It is also possible to make some qualitative statements beyond the mean-field approximation in the vicinity of a quantum critical point separating equilibrium superfluid and insulating phases. Thus we can still expect that both the tunneling action and the thermal activation barrier vanish at

$$p \sim \frac{1}{\xi}. \tag{97}$$

On the other hand, quite generally $1/\xi \sim \lambda^{\nu}$, where ν is a critical exponent [25] and λ is a tuning parameter across the transition, say deviation of the interaction U or hopping J from the critical point. In the one-dimensional case $\nu=\infty$ [51] [more precisely for the Kosterlits-Thouless transition $\xi \propto \exp(b/\sqrt{\lambda})$, where b is some constant]. In two and three dimensions the quantum critical point is characterized by the universality class of the classical xy model in one dimension higher and the corresponding critical exponents are $\nu \approx 0.67$ at $d=2$ and $\nu=0.5$ at $d=3$ [37]. We see that in three dimensions the mean-field description gives the correct value of ν. Also, quite generally, we can argue that the action (70) and the energy (73) remain valid near the quantum critical point, but with constants C and C' being renormalized,

$$C \propto \xi^{d+z-4}, \quad C' \propto \xi^{d-4}. \tag{98}$$

This in turn implies that near the quantum critical point $\lambda \ll 1$ we get

$$S_d \approx \lambda^{\nu(3/2-z)} A_d (B_d \lambda^{\nu} - p)^{5/2-d},$$
$$E_d \approx JNA'_d \lambda^{\nu/2} (B'_d \lambda^{\nu} - p)^{7/2-d}, \tag{99}$$

where A_d, A'_d, B_d, and B'_d are nonuniversal numbers. In the nongeneric commensurate case, which we are mostly interested in here, $z=1$. The scaling form above agrees with the mean-field results ($\nu=1/2$) obtained earlier. Despite quantitative difference between the correct and mean-field scaling in one and two dimensions, the qualitative features of the nonequilibrium phase transition discussed after Eqs. (92) and (96) remain intact.

V. DYNAMICS OF THE DECAY: INFLUENCE OF THE CONFINING POTENTIAL

A. Underdamped versus overdamped dynamics

As we showed above, quantum or thermal fluctuations lead to the broadening of the dynamical phase transition. However, this does not imply that within a single experimental run a gradual current decay will be necessarily detected as the system is slowly tuned through the crossover region. The tunneling or the thermal activation times define a probability of generating a single phase slip. Once created the phase slip can either decay into phonon (Bogoliubov's) modes and bring the system to a next metastable minimum with a lower current, or this phase slip can trigger the current decay in the whole system. This situation is analogous to the motion of a particle on a tilted washboard potential with friction (see Fig. 7). If the friction is large enough (or the tilt is small) then the particle, after it tunnels, will be stuck in the next minimum. On the other hand in the frictionless case a single tunneling event will cause accelerated motion of the particle through the whole lattice. In a closed system these two regimes are well defined because the damping of the phase-slip motion comes from the internal degrees of freedom, which are completely described by the equations of motion. To see which of the regimes is realized in our systems within the classical thermal decay mechanism we numerically solve Gross-Pitaveskii equations of motion for an array of condensates. We start from a uniform current state. To have a current decay we add small fluctuations to the initial values of the classical fields. This is similar to starting from a thermal state. Since we cannot change the internal friction, instead we consider two different tilts. In Fig. 8 we plot the computed current versus time for a one-dimensional array of $M=200$ sites with periodic boundary conditions. The initial state is the noninteracting $U=0$ condensate with a given phase gradient p (specifically $p=2\pi/5$ and $p=\pi/10$) and unit hopping. It is clear from the figure that we have an overdamped case for the smaller current case, where the phase slips occur one by one. On the other hand, for the larger current a single phase slip generates immediate current decay in the whole sample and this corresponds to the underdamped regime. We will not attempt here to find the pre-

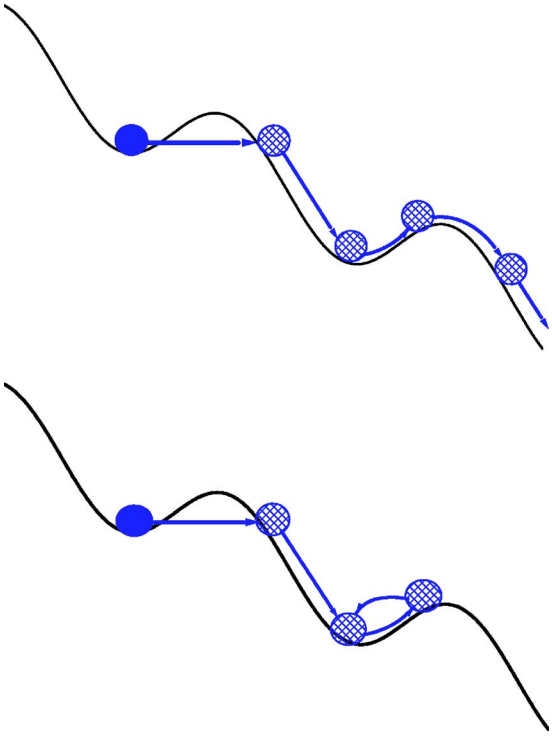

FIG. 7. Possible motion of a particle after a tunneling event in a tilted washboard potential if the friction is small (left) and if the friction is large (right). Instead of changing the friction, one can vary the tilt. It is clear that reducing the tilt is similar to increasing the friction.

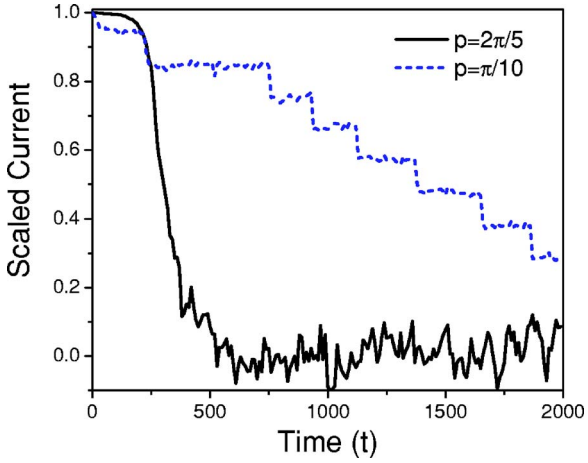

FIG. 8. Current (scaled to one at $t=0$) versus time for a one-dimensional periodic array of 200 sites with two different initial phase gradients. Here and in the following graphs time is dimensionless. Its units are set by the inverse units of couplings J and U. The evolution is determined solving equations of motion (9) with constant hopping amplitude $J=1$ and interaction increasing in time $U=0.01\tanh 0.01t$ for $p=2\pi/5$ and $U=\tanh 0.01t$ for $p=\pi/10$. To get the current decay we add small fluctuations to the initial values of the classical fields $\psi_j(t=0)$.

cise boundary between the two scenarios, since it is not the purpose of our paper. We would like to emphasize that near the mean-field instability the system is always underdamped, while if the current decays at small p the motion is overdamped. These considerations agree with the experimental observations [17,24]. We checked that the situation is similar in other spatial dimensions. Thus if the current decays close to the mean-field instability, then in a given experiment one will observe a sharp transition from the superfluid to the insulating regime. However, the precise point, where the current decays will depend on the details of the experiment, for example on the rate of change of external parameters like tunneling and interaction or on the rate of change of the phase gradient p if the system is accelerated. On the other hand, in the absence of any fluctuations the transition is very sharp and always occurs at $p=\pi/2$. We can also perform a similar analysis close to the SF-IN transition. The qualitative result that close to the modulational instability the phase-slip motion is underdamped remains correct. However, we should stress that in one and two dimensions broadening of the mean-field transition is very strong and the actual decay may occur very far from the critical current. In this case an overdamped scenario should be realized.

Unfortunately we cannot simulate the dynamics of the decay due to quantum tunneling. However, we would like to argue that near the critical current the fate of quantum and thermal phase slips is identical. This is because the tunneling (activation) barrier is very narrow and the classically allowed motion after the tunneling event starts very close to the maximum of the barrier (see Fig. 7).

We have to make another important remark that if the motion of phase slips is underdamped then in a truly infinite system the current state is always unstable. Indeed the probability of a phase slip is proportional to the system size M. If it causes the current decay in the whole system, then obviously a uniform current state cannot exist. However, in finite-size systems these effects are not so crucial, because the decay probability depends exponentially on the couplings and the current but only linearly in the system size. So the phase diagram plotted in Fig. 5 is quite robust to changes in M.

B. Decay in a parabolic trap

If in addition to the optical lattice potential the condensate is placed into a parabolic trap, then even at the classical (Gross-Pitaevskii) level the condensate momentum is not a conserved quantity. In a typical experiment, where the SF-IN transition is probed, the lattice potential is slowly ramped up resulting in hopping amplitude going down. In Appendix C we show that in this case the amplitude of momentum oscillations increases in time: $p\propto[1/J(t)]^{1/4}$ [see Eq. (C13)]. If we ignore completely the effects of quantum fluctuations, then for arbitrarily small initial displacement the condensate momentum will ultimately exceed the critical value of $\pi/2$ and the condensate motion will become unstable. If this happens before the quantum fluctuations become significant, this effect will dominate the SF-IN transition. In Fig. 9 we show the time evolution of the center-of-mass momentum p_{cm}

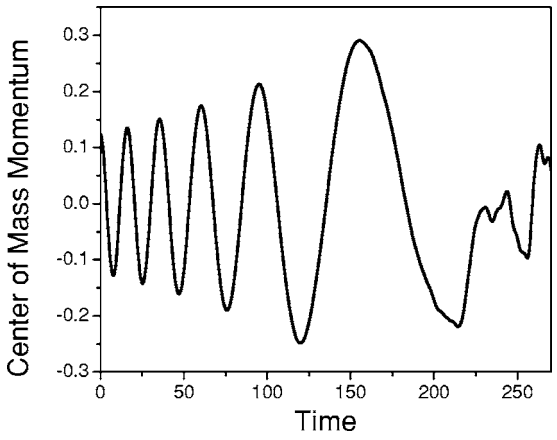

FIG. 9. Center-of-mass momentum (in the units of π per lattice site) versus time for a two-dimensional condensate in a parabolic trap with hopping amplitude decreasing in time: $J(t)=2.5\exp(-0.01t)$. The other parameters are $U=1$, number of atoms per central site $N_0=1.5$, strength of the confining potential $k=0.02$.

$=\Sigma_p p\, n_p/\Sigma_p n_p$ of the condensate in a trap using Gutzwiller approximation. Here $n_p=\Sigma_{j,l}\langle a_j^\dagger a_i\rangle\exp[ip(l-j)]$ is the momentum distribution function. The condensate initially in equilibrium is given a small momentum boost. In agreement with our expectations the amplitude of momentum oscillations grows in time. We note that at the same time the condensate velocity $v(t)\propto\sqrt{J(t)p(t)}$ decreases with time. This behavior continues until the momentum exceeds a critical value, where the condensate motion becomes chaotic.

One can avoid complications related to the nonconservation of the amplitude of momentum oscillations by tuning the interaction strength rather then the hopping amplitude. In this case one can directly probe the boundary separating stable and unstable motion of condensates at a given condensate momentum. Another important feature, which distinguishes trapped condensates from homogeneous systems, is the spatial variation of the density. Thus if the density profile is smooth enough, the condensate motion becomes unstable first near the edges where $N\approx 1$. In the center of the trap the current decays at higher interactions. As we argued earlier in this section, in homogeneous systems the motion of phase slips is underdamped near the instability, i.e., a single phase slip triggers current decay in the whole system. We can expect the same to be true in a trap as long as the mean occupation number in the central site N_0 remains close to unity. On the other hand, if $N_0\gg 1$ then it is intuitively clear that phase slips occurring near the edges cannot destabilize the motion of the bulk of the condensate, which is very far from the instability. To verify this reasoning numerically we again employ Gutzwiller approximation. In Fig. 10 we plot the momentum oscillations of a two-dimensional condensate versus time. We set the hopping amplitude $J=1/4$ while increasing the interaction linearly in time: $U(t)=0.01t$. The simulations are performed on a lattice of dimensions 120×60 with global trapping potential $V(j_x,j_y)=0.01(j_x^2+j_y^2)$. We consider two different filling factors in the central site $N_0=1.5$ and $N_0=3$. It is obvious that the onset of instability in both cases occurs at roughly the same interaction

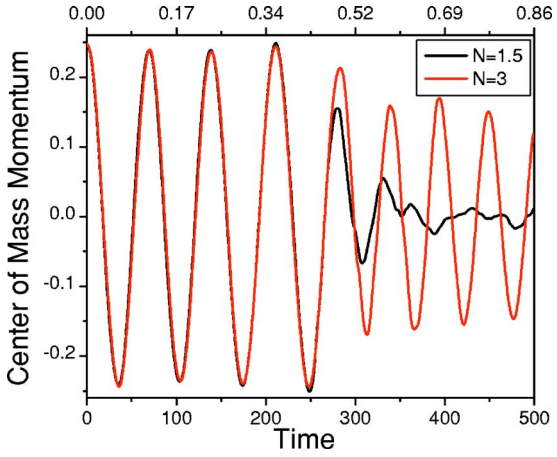

FIG. 10. Time dependence of the condensate momentum in a two-dimensional harmonic trap with different filling factors per central site.

strength (which is close to the uniform result at filling factor $N=1$). However, while the motion becomes chaotic very fast for $N_0=1.5$, there is a very gradual decay of momentum oscillations at larger filling $N_0=3$. In agreement with our expectations this indicates that an overdamped current decay is realized in the latter case.

VI. LOSS OF COHERENCE IN THE NONEQULIBRIUM PHASE TRANSITION

The superfluid–to–Mott-insulator transition at equilibrium is a continuous quantum phase transition. As such, it is expected to be reversible. That is, if we tune through the transition and then back to the initial state slowly enough, we would recover arbitrarily large fractions of the superfluid density [52].

With finite current the situation is markedly different. We envision the following experimental procedure. (i) The condensate is boosted to small but finite velocity (dipole oscillation in a trap). (ii) An optical lattice is turned on adiabatically, until the system passes the line of instability (see Fig. 11), and then slowly turned off. Finally the atoms are released from the trap, and their final momentum distribution is measured and compared to the initial one.

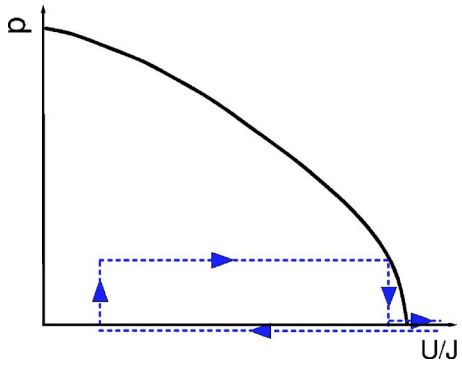

FIG. 11. Possible experimental sequence to observe a superfluid-insulator transition in a moving condensate.

The current carrying state has a finite energy, which is released into the system when the current decays. Since the system is nonintegrable, it is reasonable to assume that the energy associated with the supercurrent is released in the form of incoherent excitations, which eventually thermalize. If now the system parameters are changed sufficiently slowly, the subsequent evolution of the system is adiabatic conserving the entropy of the system. Thus the entropy change following the current decay, may be used to obtain the depletion of the superfluid in the final state of the system. We would like to emphasize that these assumptions apply if the parameters of the system change not too fast, so that the current decays in a quasistatic regime. Otherwise the current decay and the entropy release are not governed by the properties of the transition point and the actual time-dependent problem has to be solved.

The temperature of the equilibrium state reached following the current decay, and before the system parameters had a chance to change appreciably, may be calculated by equating the energy of the superflow, prior to its decay, with the internal energy of the system in the new thermal equilibrium:

$$\delta\epsilon(p) = \frac{1}{M}\sum_{\mathbf{q}} \frac{\omega_q}{e^{\beta\omega_q} - 1}. \tag{100}$$

The low-energy excitations in the superfluid state are linearly dispersing sound modes with $\omega_{\mathbf{k}} \approx ck$. Substituting this in Eq. (100), we can solve for the temperature to obtain

$$T = A_d c^{d/(d+1)} \delta\epsilon(p)^{1/(d+1)}, \tag{101}$$

where

$$A_d = \left(\frac{(2\pi)^d}{\Omega_d d\,!\,\zeta(1+d)}\right)^{1/(d+1)}, \tag{102}$$

Ω_d is the surface area of the d-dimensional unit sphere, and ζ stands for the Riemann zeta function. Accordingly, the entropy of this thermal state is given by

$$\mathcal{S} = \frac{\delta\epsilon(p)}{T} - \sum_{\mathbf{q}} \ln(1 - e^{-\beta\omega_q}) \approx A_d^{-1}\left(\frac{\delta\epsilon}{c}\right)^{d/(d+1)} \frac{d+1}{d}. \tag{103}$$

As argued above, we can use this entropy to calculate the condensate depletion in the final state.

Let us apply this procedure assuming that the current decays via the instability in the vicinity of the Mott transition. Though we do the calculation for all dimensions, one should note that such a scenario is particularly relevant for a three-dimensional optical lattice. According to Sec. V, in lower dimensions the current will most probably have decayed due to fluctuations before reaching the instability.

The energy per site of a state near the Mott transition according to the Ginsburg-Landau model (see Appendix A) is given by

$$\epsilon = \frac{JN}{2duV}\int d^d x \left[|\nabla\psi|^2 - \xi^{-2}|\psi|^2 + \frac{1}{2}|\psi|^4 \right]. \tag{104}$$

Substituting the field corresponding to the current carrying state, $\psi = \sqrt{\xi^{-2} - p^2}\, e^{ipx}$, we obtain

$$\delta\epsilon = \epsilon(p) - \epsilon(0) = \frac{JN}{2du}\left(\xi^{-2} - \frac{1}{2}p^2\right)p^2. \tag{105}$$

Recall that our proposed experiment maintains constant p and changes the dimensionless interaction, and hence also ξ, by increasing the lattice intensity. The current decays when the instability is reached, i.e., when $\xi^{-2} = \xi_c^{-2} = 3p^2$, at which point the energy per site is

$$\delta\epsilon \approx \frac{JN}{2d}\frac{5}{2}p^4. \tag{106}$$

Thus the energy released following decay via the instability at phase gradient p is $\propto p^4$. Using Eq. (103) and the sound velocity near the transition $c = 2JN\sqrt{2d}$ we get the increase of entropy per site:

$$S = \frac{d+1}{dA_d}\left(\frac{5}{4(2d)^{3/2}}\right)^{d/(d+1)} p^{4d/(d+1)}. \tag{107}$$

In three dimensions, this gives $S_{3d} \approx 0.16p^3$. With such a small increase of entropy we anticipate that the irreversibility, as manifest in the unrecovered condensate fraction, would also be small for low initial currents. Perhaps the simplest way to see this is to slowly reduce the lattice intensity until the atoms are very weakly interacting before releasing to measure the momentum distribution. In this case the elementary excitations have a quadratic dispersion $\omega_{\mathbf{k}} = \alpha k^2$. In general this assumption is not necessary and one can use the full Bogoliubov spectrum. However, qualitatively the result remains the same. A nice feature of the quadratic dispersion is that the thermal depletion is simply related to the entropy, which is given by

$$S = \left(\frac{d+2}{d}\right)\frac{E}{T} = \frac{\Omega_d}{(2\pi)^d}\left(\frac{d+2}{d}\right)\left(\frac{T}{\alpha}\right)^{d/2} I_d, \tag{108}$$

where

$$I_d = \int_0^\infty dx \frac{x^{d+1}}{e^{x^2} - 1}. \tag{109}$$

The thermal depletion, on the other hand, is

$$n_T = \frac{1}{V}\sum_{\mathbf{q}} \frac{1}{e^{\alpha q^2/T} - 1} = \left(\frac{d}{2+d}\right)\frac{S}{I_d}\int_{x_0}^\infty dx x^{d-1}\frac{1}{e^{x^2} - 1}, \tag{110}$$

where x_0 depends on the small momentum cutoff determined by the system size (i.e., $x_0 \sim L\sqrt{\alpha/T}$). In three dimensions the last integral is convergent and we get

$$n_T^{3d} = \frac{2\zeta(3/2)}{5\zeta(5/2)}S \approx 0.78S. \tag{111}$$

Thus in three dimensions the number of excited quasiparticles, or condensate depletion, is a direct measure of the entropy.

In one and two dimensions, on the other hand, the integral has an infrared divergence. Of course this is simply a restatement of the well-known fact that a true condensate in free space at finite temperature does not exist below three dimen-

sions. In practice, the divergence is cut off by the system size and one can define the notion of a quasicondensate. In two dimensions where the divergence is only logarithmic,

$$n_T^{2d} \approx \frac{6}{\pi^2} S \ln(L\sqrt{S}), \tag{112}$$

and finally in one dimension

$$n_T^{1d} \approx 0.04 S^2 L. \tag{113}$$

Instead of the system size the cutoff may come from the finite momentum resolution (Δp) of the experimental apparatus. In general the momentum cutoff will be determined by the minimum of L and $1/\Delta p$. We see that below three dimensions condensate depletion due to thermal decay at small currents is more pronounced and easier to detect than at $d=3$.

The situation is different if the current decays at smaller interaction strengths (smaller lattice intensity) at large currents. The energy of the current state may then be calculated from the Gross-Pitaevskii energy functional:

$$E = -J\sum_{\langle ij\rangle} (\psi_i^\star \psi_j + \psi_j^\star \psi_i) + \frac{U}{2}\sum_i |\psi_i|^4. \tag{114}$$

Substituting $\sqrt{N}e^{ipx_j}$ for ψ_j we find $\delta\epsilon = 4JN\sin^2(p/2)$. Together with Eq. (103) and using the sound velocity $c = \sqrt{2UJN}$ we get the entropy increase per site:

$$S_{1d} \approx 2.4\left(\frac{JN}{U}\right)^{1/4} \sin\frac{p}{2}, \tag{115}$$

$$S_{2d} \approx 2.2\left(\frac{JN}{U}\right)^{1/3} \sin^{4/3}\frac{p}{2}, \tag{116}$$

$$S_{3d} \approx 2.2\left(\frac{JN}{U}\right)^{3/8} \sin^{3/2}\frac{p}{2}. \tag{117}$$

Evidently the irreversibility is stronger and easier to detect if the current decays at smaller interaction strengths.

VII. EXACT RESULTS IN SMALL SYSTEMS

In this section we present results of exact dynamics in small one-dimensional systems. We will assume that we have a periodic one-dimensional array of M sites containing N particles. At $t=0$ we assume that interactions are absent and the system is placed in the uniform current state, described by the wave function,

$$|\psi\rangle = \frac{1}{\sqrt{N!}}\left(\frac{\sum_{j=0}^{M-1} a_j^\dagger e^{ipj}}{\sqrt{M}}\right)^N |0\rangle, \tag{118}$$

where $|0\rangle$ is the no-particle vacuum. This state is an exact eigenstate of the noninteracting system. Now we slowly turn on interactions driving the system closer to the insulating regime and then gradually turn them off. The latter step is necessary to check whether we have reversible dynamics or irreversible current decay. Although in real experiments it is rather tunneling not the interaction which is changed in time, this does not make any qualitative difference in uniform systems. If the interaction is ramped up infinitesimally slowly, then any finite system will remain within a particular energy eigenstate and the evolution will be always reversible. However, the energy splitting between the many body levels decreases exponentially with the system size and the number of particles. So practically even in relatively small systems, one can study dynamics, which is slow with respect to the characteristic time scales (like period of Josephson oscillations), but very fast with respect to the inverse many-body energy spacing. To make this point more transparent we plot in Fig. 12 the energy spectrum versus U/J for a particular system of a periodic array consisting of six sites and containing six particles. The size of the Hilbert space here is already quite big: $\mathcal{N}=11!/(6!5!)=462$. It is obvious from the figure that while the ground state is well separated from the continuum at all interaction strengths, the excited states experience many level crossings. So it is nearly impossible to be in or close to the adiabatic regime unless the system is in the ground state.

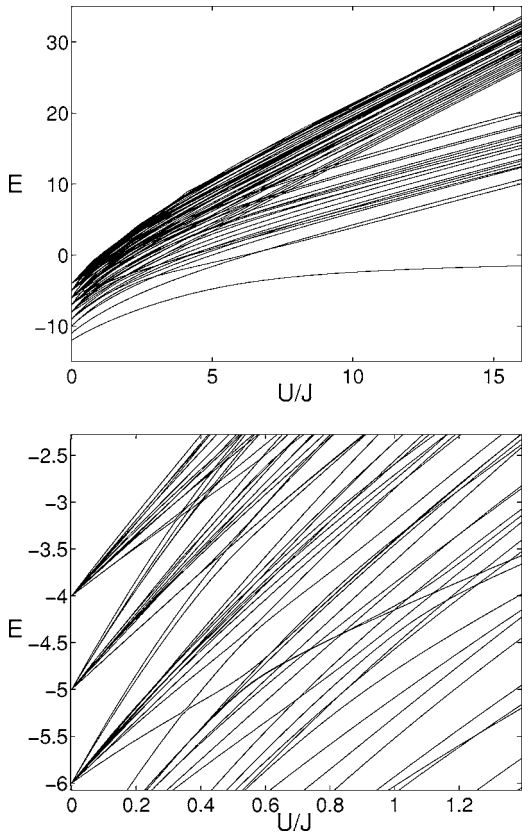

FIG. 12. First one-hundred energy levels of the spectrum in a periodic array of six sites containing six particles (top) and zoom of the energy spectrum around the current carrying state with $p=\pi/6$ (bottom). It is clear that while the ground state is well separated from the continuum for all interaction strengths, the excited many-body states are completely mixed. So it is nearly impossible to be in the adiabatic regime unless the system is initially in the ground state.

Let us assume that the Hamitonian is described by Eq. (2), where the interaction strength changes in time according to

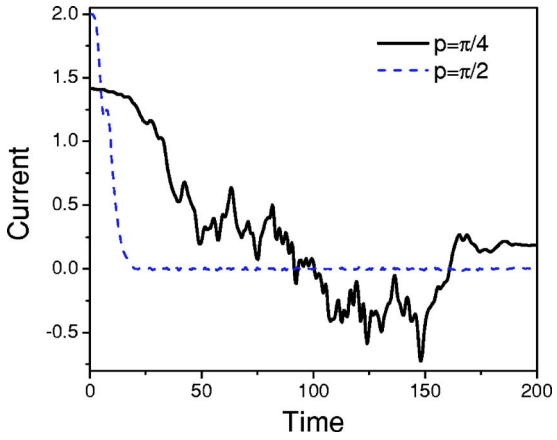

FIG. 13. Dependence of current on time for the system of eight sites with two particles per site. The hopping amplitude is equal to unity and is independent of time. The interaction changes in time according to Eq. (119) with $U_0=2$, $\delta=0.02$, and $T=200$.

$$U(t) = U_0 \tanh \delta t \tanh \delta(T-t), \tag{119}$$

where δ is the adiabaticity parameter, T is the duration of the time evolution, and U_0 is a prefactor setting the energy scale. We also assume that the hopping J is equal to unity and does not change in time.

In Fig. 13 we plot the current versus time for the array of eight sites with two particles per site. The two curves correspond to initial phase gradient of $\pi/4$ and $\pi/2$ per bond. The smaller current decays when the interaction becomes sufficiently large, in agreement with that this state is metastable, while the $\pi/2$ state decays almost instantly since it is classically unstable. In both cases the decay is clearly completely irreversible. To make the final point more transparent we also plot momentum distribution as a function of time for the same parameters in Fig. 14. The curve corresponding to a zero current state shows reversible behavior, suggesting that

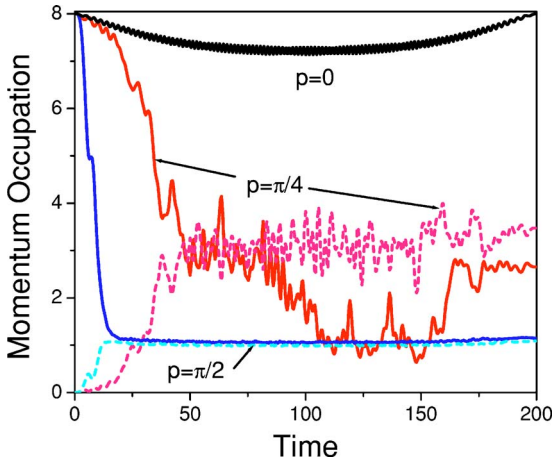

FIG. 14. Occupation of momentum states as a function of time for different current carrying states. Solid lines correspond to the occupation of momentum p equal to the initial phase gradient in the system. The dashed lines are the occupations of the zero-momentum state. The parameters are the same as in Fig. 13.

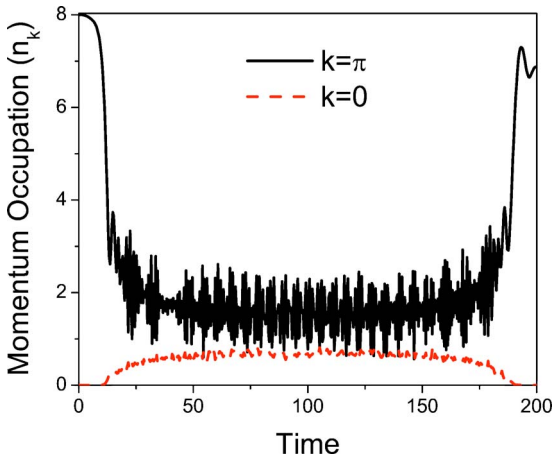

FIG. 15. Occupations of the $k=0$ and $k=\pi$ states for the state with initial phase gradient $p=\pi$. Here the interaction changes in time according to Eq. (119) with $U_0=1$, $\delta=0.02$, and $T=200$.

the interaction indeed changes slowly enough so that the system is in the adiabatic limit. Note that even at the peak interaction strength, the system is still far from the insulating state, as evident from the very small depletion of the $p=0$ state. Nevertheless, because the smallest phase difference per site achievable in an array of size 8 is still quite large ($p=\pi/4$), this interaction is sufficient to drive current decay. Indeed the curve corresponding to initial phase gradient of $\pi/4$ clearly displays metastable behavior, with current decaying after some delay. In the new steady state reached, occupation of zero momentum builds up suggesting that it corresponds to a thermal distribution with no macroscopic current, but with some residual phase coherence. The state with phase gradient $p=\pi/2$, by contrast, seems to decay into a high-temperature state, without visible phase correlations. Indeed, occupation of momenta zero and $\pi/2$ are equal to unity as expected if the phases were completely random. It is peculiar that there are only very weak fluctuations of the momentum distribution in this state. This should be contrasted with the rather large fluctuations seen following decay of the $\pi/4$ current state.

Finally, condensates sustaining phase gradients $p>\pi/2$ are classically unstable, and are expected to decay rapidly, resulting in even higher temperature than for the $\pi/2$ state. The $p=\pi$ state is an interesting exception to this rule. As argued in Refs. [35,41], this state evolves into a maximally entangled Schrödinger-cat-like state, which is robust to weak perturbations in small systems. Physically this happens because the π state in the noninteracting case is the most excited state in the system. In the absence of energy relaxation the system remains in the most excited state under slow perturbations in the same way as it does in the ground state. And therefore we can expect reversible behavior of the phase coherence. We plot the corresponding momentum distribution for this state in Fig. 15. Although for the intermediate times the evolution looks completely chaotic, once the interaction is reduced back to zero the momentum occupancy at $k=\pi$ reaches almost the maximum possible initial value suggesting only a small amount of excitations in the system.

Unfortunately, doing exact numerical simulations we are quite limited by the total system sizes and the number of

particles. Also we can address only one-dimensional systems. Therefore we cannot directly test the phase diagram and decay rates derived in the previous sections. Nevertheless, we would like to point out that the numerical results are in excellent qualitative agreement with our predictions.

VIII. SUMMARY AND EXPERIMENTAL IMPLICATIONS

In summary we emphasize two important predictions of this work. In Sec. III we derived a mean-field phase diagram for the stability of a moving condensate. In Sec. IV we investigated the effect of quantum and thermal fluctuations, which lead to broadening of the nonequilibrium transition.

We showed that the mean-field transition interpolates between the classical modulational instability, which occurs at phase gradient $p=\pi/2$ deep in the superfluid regime and the equilibrium ($p=0$) transition to the Mott insulating phase at strong interactions. The dynamical transition is of first order (i.e., irreversible) at any nonzero current, contrary to the second-order transition at equilibrium. Thus if one starts from a current state and slowly drives the system towards the insulating regime, e.g., by ramping up the lattice potential, then after crossing the transition boundary the current decays irreversibly, releasing the energy of the coherent motion into heat. Plotting the location of the nonequilibrium transition as a function of the current and extrapolating the curve into the static regime $p=0$ is a way to accurately determine the position of the equilibrium SF-IN transition.

The mean-field theory does not take into account quantum tunneling and thermal activation of phase slips. These induce decay of supercurrent, even before the classical equations of motion become unstable. We calculated the asymptotic decay rates near the mean-field instability in two regimes: (i) deep in the superfluid regime and (ii) close to the equilibrium Mott transition.

In a three-dimensional optical lattice the broadening of the transition due to these effects is found to be small in all cases. In particular we find a discontinuity in the current decay rate across the mean-field transition for small currents at zero temperature (close to the equilibrium Mott transition). Thus the dynamical transition survives the effect of quantum fluctuations in this case. We predict that a sharp dynamical superfluid-insulator transition would be seen at small currents at a critical interaction strength (or lattice depth).

In one and two dimensions, on the other hand, quantum and thermal phase slips lead to substantial broadening of the transition, especially when the average site occupation $N \sim 1$. Then we expect the current to decay well before the dynamical instability is reached. Indeed, in a recent experiment [24] strong damping was detected at currents much smaller than that given by the Gross-Pitaevskii modulational instability. In addition the observed dependence of the damping rate on the lattice depth potential was very smooth. This is in line with our prediction of a the large broadening of the mean-field transition by quantum fluctuations and should be contrasted with the Gross-Pitaveskii predictions of a sharp transition. It is also consistent with earlier numerical results by one of us [22].

The experimental results [24] do not by themselves prove that quantum rather than thermal fluctuations are responsible for the observed damping. Here we estimate the crossover temperature from thermal to quantum dominated decay to be of order the Josephson frequency $T^\star \approx \sqrt{JUN}/k_B$. The experiment is therefore likely to be dominated by quantum phase slips. To verify this conclusion, one could measure, e.g., the damping as a function of temperature and observe a saturation of the rate around $T^\star$.

One perhaps surprising experimental observation was that in the overdamped regime (i.e., at high optical lattice potential) the condensate was essentially localized in a tilted lattice, while it still exhibited sharp coherence peaks [24]. A possible explanation is the effect of the inhomogeneous density in a harmonic trap, which we discussed in Sec. V. Indeed, in the overdamped regime one expects no suppression of phase slip tunneling at the edges of the condensate, where $N \approx 1$. This implies that the phase at the edges fluctuates very wildly and the edge atoms are localized. On the other hand, in the middle of the condensate, where the mean number of particles per site is larger, the system is far from the mean-field transition and phase slips are relatively costly. As a result, the edges of the condensate create an effective potential barrier stopping the motion of the rest of the system, which retains phase coherence.

Our results are consistent with another recent experiment, where the superfluid decay was measured as a function of the condensate velocity in a one-dimensional optical lattice [53]. There the average number of bosons per site was large and quantum fluctuations negligible. At low temperature a dynamical localization transition consistent with Gross-Pitaveskii predictions was observed. However, at relatively high temperatures, the motion became unstable at much lower quasimomentum. This observation qualitatively agrees with the decay mechanism due to thermal phase slips considered in the present work.

We also presented exact numerical simulation of small one-dimensional systems. These were in qualitative agreement with the physical picture discussed in the paper. For example, we demonstrated that at nonzero current the transition is irreversible. We also find that in a periodic chain of eight sites, the current state with $p=\pi/4$ decays only at some finite interaction strength, while at $p=\pi/2$ the decay occurs almost instantly. An important exception is the case with $p=\pi$, where the evolution is reversible (see also Ref. [52]). A quantitative comparison of the exact numerical results with our predictions is not possible because of strong finite-size effects in the exact simulations.

Note added. Recently, two preprints appeared [55,56] which address the experiment by Fertig *et al.* [24]. There, the damping was attributed to single-particle Bloch oscillations in the free fermion representation of the bosons in the limit of strong interactions. This effect can also be understood in the Boson language. If the number of particles in the trap is small, the system reaches the impenetrable boson regime while not yet insulating. Indeed one can easily transfer a boson from a filled to an empty site near the edge of the system. If the tunneling amplitude (J) is larger than the single-particle energy near the edge of the cloud $J > kN_t^2/8$ then the created hole is delocalized through the whole system and the state is not insulating. Here $kj^2/2$ is the confining potential of the trap and N_t is the total number of particles,

which equals the system size in the Fermionized regime. The hard-core constraint in turn requires that $U \gg J$. Therefore if $U \gg kN_t^2$ and we gradually decrease J then indeed the system first goes to Fermionized delocalized regime $U \gg J \gg kN_t^2$ and only if J is decreased further it becomes localized. On the other hand, if the total number of bosons is large $U \ll kN_t^2$, which is the case close to the thermodynamic limit, then the edge excitations in the Fermionized regime are always localized and thus unimportant for the macroscopic properties of the system.

We emphasize that if the first (i.e., small particle number scenario) is realized, then after the trap minimum is displaced, the particles will essentially undergo Bloch oscillations with different frequencies resulting in a damped center-of-mass motion [55]. In this scenario there is no real energy relaxation of the center of mass and it will saturate at a displaced position [56]. In the second case $U \ll kN_t^2$ the system undergoes a Mott transition when the impenetrable regime is reached and the edge Bosonic excitations can result only in a tiny center-of-mass displacement vanishing in the thermodynamic limit. The damping prior to the Mott transition in this case occurs via the mechanisms discussed in this paper, i.e., the current decay is irreversible and results in energy relaxation of the center-of-mass motion, which will eventually slide to the minimum of the trap. This seems to be the case realized in the experiment of Ref. [24].

We also mention that the single-particle Bloch physics will dominate the decay mechanisms studied here if the Bloch oscillation, which frequency is equal to the single-particle energy separation between the nearest sites due to external potential, is longer than the Josephson oscillation.

ACKNOWLEDGMENTS

We would like to acknowledge D.-W. Wang for helpful discussions and collaboration on related work. This work was supported by NSF Grant Nos. DMR-01328074, DMR-0233773, DMR-0231631, DMR-0213805, and PHY-0134776, the Sloan and the Packard Foundations, and by Harvard-MIT CUA.

APPENDIX A: DERIVATION OF A GINZBURG-LANDAU ACTION NEAR THE SUPERFLUID-INSULATOR TRANSITION

A derivation of a Ginzburg-Landau action near the superfluid-insulator transition was outlined in Ref. [38]. For convenience we present the full derivation in this appendix.

Let us choose the energy of a single site with integer N atoms, as the zero of energy. Then the Hamiltonian of the boson Hubbard model (1) assumes the form

$$H = -J\sum_{\langle ij\rangle}(a_i^\dagger a_j + \text{H.c.}) + \sum_i \frac{U}{2}(n_i - N)^2 - \mu(n_i - N). \tag{A1}$$

Close to the superfluid-insulator transition, the particle number fluctuation is small. It is then possible to consider a subspace allowing only occupations of $N-1$, N, and $N+1$ atoms per site. This reduced Hilbert space is conveniently described by a (overcomplete) basis of product states:

$$|\Omega\rangle = \prod_j \{\cos(\theta_j/2)|N\rangle_j + e^{i\eta_j}\sin(\theta_j/2)[e^{i\varphi_j}\sin(\chi/2)|N+1\rangle_j + e^{-i\varphi_j}\cos(\chi/2)|N-1\rangle_j]\}. \tag{A2}$$

We shall use these states to construct a path integral for the evolution operator. The derivation can be carried out for arbitrary N, but for simplicity of presentation we take $N \gg 1$. The first step is to prove a resolution of identity:

$$\int_0^\pi d\theta \int_0^\pi d\chi \int_0^{2\pi} d\varphi \int_{-\pi/2}^{\pi/2} d\eta \mathcal{M}(\Omega)|\Omega\rangle\langle\Omega| = \mathcal{I}. \tag{A3}$$

We shall now find a suitable integration measure $\mathcal{M}(\theta)$, which is a function of θ only. Substituting $\mathcal{M}(\theta)$ in Eq. (A3), we can integrate over η, φ, and χ, which kills off the cross terms so that Eq. (A3) reduces to

$$\mathcal{I} = 2\pi^3 \int_0^\pi d\theta \mathcal{M}(\theta)\left\{\cos^2\frac{\theta}{2}|N\rangle\langle N| + \frac{1}{2}\sin^2\frac{\theta}{2}(|N+1\rangle\langle N+1| + |N-1\rangle\langle N-1|)\right\}. \tag{A4}$$

The measure $\mathcal{M}(\theta)$ must enforce the identity between the diagonal matrix elements, so that

$$\int_0^\pi d\theta \mathcal{M}(\theta)\left(\cos^2\frac{\theta}{2} - \frac{1}{2}\sin^2\frac{\theta}{2}\right) = 0 \tag{A5}$$

or equivalently

$$\int_0^\pi d\theta \mathcal{M}(\theta)(1 + 3\cos\theta) = \int_{-1}^1 dy \frac{\mathcal{M}(y)(1+3y)}{\sqrt{1-y^2}} = 0, \tag{A6}$$

where $y = \cos\theta$. This requirement is satisfied by $\mathcal{M}(\theta) = C\cos\theta(3\cos\theta - 1)$, since it ensures that the integrand is an antisymmetric function of $\cos\theta$. The constant $C = \pi^{-4}$ is determined from normalization. Since we are interested in the vicinity of the transition at $\theta = 0$, where the measure $\mathcal{M}$ changes slowly, it is safe to replace it with a constant.

It is also straightforward to calculate the Berry phase,

$$\left\langle \Omega \left| \frac{d}{dt} \right| \Omega \right\rangle = i\sum_j \sin^2(\theta_j/2)(\dot{\eta}_j - \cos\chi_j\dot{\varphi}_j) \equiv -i\Upsilon(t). \tag{A7}$$

Equations (A3) and (A7) are the necessary ingredients for the path-integral representation of the evolution operator:

$$\mathcal{U}(t) = \int \mathcal{D}\Omega \exp\left\{i\int_0^t dt'[\Upsilon(t') - \mathcal{H}(t')]\right\}, \tag{A8}$$

where the classical Hamiltonian is given by

$$\mathcal{H} = \langle \Omega|H|\Omega\rangle = \sum_i \sin^2(\theta_i/2)\left(\frac{U}{2} - \mu\cos\chi_i\right) - 2JN\sum_{\langle ij\rangle}\rho_i\rho_j[c_ic_j\cos(\eta_j - \eta_i + \varphi_i - \varphi_j) + s_is_j\cos(\eta_j - \eta_i + \varphi_j - \varphi_i) + c_is_j\cos(\eta_i + \eta_j + \varphi_j - \varphi_i) + s_ic_j\cos(\eta_i + \eta_j + \varphi_i - \varphi_j)]. \quad \text{(A9)}$$

Here we introduced the notations $c_i \equiv \cos(\chi_i/2)$, $s_i \equiv \sin(\chi_i/2)$, and $\rho_i \equiv (1/2)\sin\theta_i$. It is important to note that the dynamics defined by Eqs. (A7) and (A8), consists of two pairs of conjugate variables. The average offset from integer density is conjugate to the phase φ, while the second moment (i.e. the number fluctuation) is conjugate to η.

At fillings close to integer, the minimum classical energy is reached in a uniform state with χ close to $\pi/2$ and $\eta=0$. We therefore expand the action to leading order in $\sigma_i=\pi/2-\chi_i$ and η_i. In addition we expand up to quartic order in ρ, and anticipating a diverging length scale at the transition, take the continuum limit of the action via a gradient expansion

$$S \approx \int dt'd^dx[\rho^2\sigma(\dot{\varphi}+\mu) - \rho^2\dot{\eta} - 2JN[(\nabla\rho)^2 + \rho^2(\nabla\varphi)^2] + 4JNd(1-u)\rho^2 - 4JNd\cdot u\rho^4 - 2JNd\rho^2(2\eta^2+\sigma^2/2)], \quad \text{(A10)}$$

where $u=U/8JNd$. We can now integrate over the gaussian fields η and σ to obtain a Ginzburg-Landau (GL) action:

$$S = \int dt'd^dx\left(\frac{1}{4JNd}[\dot{\rho}^2 + \rho^2(\dot{\varphi}+\mu)] - 2JN[(\nabla\rho)^2 + \rho^2(\nabla\varphi)^2] - 4JNd(1-u)\rho^2 + 4JNd\cdot u\rho^4\right)$$
$$= \frac{1}{4JNd}\int dt'd^dx[|(\partial_t + i\mu)\psi|^2 - (2JN)^2 2d|\nabla\psi|^2 + (4JNd)^2(1-u)|\psi|^2 - (4JNd)^2 u|\psi|^4], \quad \text{(A11)}$$

where $\psi \equiv \rho e^{i\varphi}$. Note that in Eq. (A10) we left out terms of the form $\rho^2(\nabla\eta)^2$ and $\rho^2(\nabla\sigma)^2$. After integrating over η and σ, these would lead to irrelevant high-order derivatives in the GL action. We can identify a sound velocity $c=2JN\sqrt{2d}$, where the lattice constant is set to $l=1$. If we now make the transformation $t\to ct$ (i.e., measure time in units of l/c), and $\psi\to\psi\sqrt{4du}$, the GL action assumes the form

$$S = \frac{1}{\alpha}\int dtd^dx|(\partial_t + i\mu)\psi|^2 - |\nabla\psi|^2 + r|\psi|^2 - \frac{1}{2}|\psi|^4, \quad \text{(A12)}$$

where $r=2d(1-u)$ and $\alpha=2u(2d)^{3/2}$. In the superfluid phase $r=\xi^{-2}$, where ξ is the mean-field coherence length. Note that the action is Lorentz invariant only at commensurate filling, where by our choice of the zero of energy for Eq. (A1), $\mu=0$. This is due to the particle-hole symmetry, which is present only at commensurate filling.

From the action (A12), we can find the deviation from commensurate filling, given by the conserved charge:

$$Q = \frac{\delta S}{\delta\mu(t)} = \frac{1}{\alpha i}\int d^dx[\psi^\star(\partial_t + i\mu)\psi - \psi(\partial_t - i\mu)\psi^\star]. \quad \text{(A13)}$$

In Eq. (A1), we chose the zero of energy such that the chemical potential is $\mu=0$ at commensurate filling N. Indeed, if we substitute $\mu=0$ in Eq. (A13) and a time-independent order parameter we get $Q=0$ as required. However, we note that the time derivative always appears in a gauge invariant combination with the chemical potential. Therefore the action (A12) and the "charge" (A13) do not depend on the particular choice of the zero of energy. In particular, for calculating the dynamics it would prove convenient to use a different gauge, applying the transformation $\psi\to\psi e^{i\phi(t)}$, $\mu\to\mu-\dot{\phi}$ with $\phi=\mu t$. This eliminates μ from the action, at the expense of imposing on the order parameter an additional time-dependent phase. The two gauges coincide at the commensurate point where $\mu=0$ and there is no time-dependent phase. At incommensurate filling, though the action seems Lorentz invariant in the new gauge, the physics is clearly not, due to the imposed time-dependent phase

We also note that in any gauge we can trace back the density parameter $\sigma=\pi/2-\chi$, appearing in the Gutzwiller states (A2). In mean-field theory, integrating out σ in Eq. (A10) simply enforces the identity $\sigma=\sqrt{8/d}(\dot{\varphi}+\mu)$. A small incommensurate filling is then given by $\sigma\rho^2$.

The Euler-Lagrange equations derived from the action in the new gauge (where μ is eliminated from the action) are given by Eq. (11), which we reproduce here for completeness:

$$\frac{\partial^2\psi}{\partial t^2} = \nabla^2\psi + r\psi - |\psi|^2\psi. \quad \text{(A14)}$$

In this gauge the density offset from integer filling is set exclusively by the initial conditions for ψ and $\dot{\psi}$ and given by

$$Q = \frac{1}{\alpha i}\int d^dx(\psi^\star\dot{\psi} - \psi\dot{\psi}^\star). \quad \text{(A15)}$$

It is easily verified that Eq. (A15) is a conserved quantity in the equations of motion (A14). This gauge choice is thus analogous to the canonical ensemble, where the particle number is fixed and is automatically conserved by the dynamics at all later times.

Before concluding this appendix let us make several notes. First, to obtain the action (70) from Eq. (A12), one has to rotate to imaginary time $t=ix_0$ and rescale length $\mathbf{x}\to\xi\mathbf{x}$ (i.e., measure length in units of the coherence length) and the order parameter $\psi\to\xi^{-1}\psi$. Then in the "canonical gauge" the action assumes the form

$$S = \frac{\xi^{d-3}}{2u(2d)^{3/2}}\int d^{d+1}x\left[|\nabla\psi|^2 - |\psi|^2 + \frac{1}{2}|\psi|^4\right], \quad \text{(A16)}$$

which is identical to Eq. (70). Second, to obtain the classical energy from Eq. (A12) in the original static gauge, we sim-

ply set time-independent fields and multiply by the energy unit c/l:

$$\mathcal{E} = \frac{JN}{2ud}\int d^dx\left[|\nabla\psi|^2 - [r + (\mu l/c)^2]|\psi|^2 + \frac{1}{2}|\psi|^4\right]. \tag{A17}$$

The average density offset form integer filling is then given by

$$\langle n - N\rangle = -\frac{\partial\mathcal{E}}{\partial\mu} = \frac{2\mu}{\alpha}|\psi|^2, \tag{A18}$$

which agrees with Eq. (A13) evaluated in the static gauge, as it should.

Another note we should make is that for low filling factors $N\sim 1$, the general form of the action remains the same, in the vicinity of the Mott transition. However, in that case, the expressions for ξ, c, and the prefactor of the action are more complicated.

APPENDIX B: DERIVATION OF THE PREFACTOR OF THE CURRENT DECAY IN A ONE-DIMENSIONAL LATTICE

Following a general theory developed in Ref. [44], in the one-dimensional case, we can find the transition rates per site Γ_- and Γ_+. These can be written as

$$\Gamma_\pm = \frac{4}{\pi\tau}\sqrt{\frac{JN}{U}}|\omega_0\omega^0_{L/2}|\prod_{n\geqslant 1}\frac{\omega^0_n}{\omega_n}\exp\left(-\frac{\Delta E_\pm}{T}\right), \tag{B1}$$

where τ is the phenomenological coupling to the bath degrees of freedom, defined in terms of dissipative Gross-Pitaveskii equations:

$$\tau\frac{\partial\psi_j}{\partial t} = \psi_{j+1} + \psi_{j-1} - \frac{U}{2J}|\psi_j|^2\psi_j + \mathcal{L}_j(t). \tag{B2}$$

Here $\mathcal{L}_j(t)$ is the Langevin noise term; ω_j and ω^0_j are the eigenvalues of the excitations of Eq. (53) around the saddle-point and metastable states, respectively. Note that both states have one zero eigenvalue due to global phase U(1) symmetry and we ignore them. The saddle-point spectrum also has one imaginary eigenvalue (ω_0) corresponding to an unstable solution of the linearized equations of motion. An extra prefactor $\omega^0_{L/2}$ comes because in the saddle-point configuration the number of solutions with real ω is smaller by 1 than in the metastable state. For simplicity we assume L to be even. Because of the absence of continuous translational symmetry, there is no second zero eigenvalue for the saddle point (compare with Ref. [31]). The eigenfunctions of small fluctuations around the metastable state are plain waves. The corresponding spectrum thus reads

$$\omega_n = 2\sqrt{2\cos p}\,\sin k_n/2, \tag{B3}$$

where $k_n = 2\pi n/L$ is the momentum, $n = 0,1,\ldots L-1$ is an integer, and L is the size of the chain.

The saddle-point solution with a single phase slip has scattering states and a bound state. The latter is described by the eigenfunction

$$\delta\phi_j = A\times\begin{cases} e^{-\kappa(j-1)} & j\geqslant 1 \\ -e^{\kappa j} & j\leqslant 0. \end{cases} \tag{B4}$$

Substituting Eq. (B4) into the linearized version of Eq. (53) we find $\kappa = \ln 3$ and $\omega_0 = 4i\sqrt{2/3\cos p}$, where we ignored a small discrepancy between p and p'.

To find the scattering states we shall seek solutions in the form

$$\delta\phi_j = Ae^{ikj} + Be^{-ikj} \tag{B5}$$

for $j = 1,2,\ldots L-1$ and $\delta\phi_0 \equiv \delta\phi_N$, where $\delta\phi_j$ is the small deviation from the saddle-point solution (54). The system of secular equations determining the wave vectors k_n reads

$$A(1 + e^{ikL} - 2e^{ik}) + B(1 + e^{-ikL} - 2e^{-ik}) = 0, \tag{B6}$$

$$Ae^{ik}(1 + e^{ikL} - 2e^{ik(L-1)}) + Be^{-ik}(1 + e^{-ikL} - 2e^{-ik(L-1)}) = 0. \tag{B7}$$

A nontrivial solution of the above system exists for k satisfying the following equation:

$$\tan\frac{kL}{2} = 2\tan\frac{k}{2}. \tag{B8}$$

Introducing the phase shift $k_n = 2\pi n/L + \delta_n/L$ we find

$$\tan\frac{\delta_n}{2} = 2\tan\left(\frac{\pi n}{L} + \frac{\delta_n}{2L}\right). \tag{B9}$$

In the limit $L\to\infty$ we get the approximate solutions for the scattering phase shifts:

$$\delta_n \approx 2\arctan\left(2\tan\frac{\pi n}{L}\right). \tag{B10}$$

The energies of the scattering states are equal to

$$\omega'_n = 2\sqrt{2\cos p'}\sin\left(\frac{\pi n}{L} + \frac{\delta_n}{2L}\right). \tag{B11}$$

Now it is straightforward to find the ratio of the products of all eigenvalues at the saddle point and the metastable state in the limit $L\to\infty$:

$$\prod_n\frac{\omega'_\mp}{\omega_n} = 3\,e^{\pm\tan p(\pi\mp 2p/2)}. \tag{B12}$$

Substituting this into the general expression (B1) we derive Eqs. (59) and (60).

APPENDIX C: GROSS-PITAEVSKII DYNAMICS OF A LATTICE CONDENSATE IN A PARABOLIC TRAP UNDER SLOW CHANGE OF THE HOPPING AMPLITUDE

In the superfluid regime the most significant effect of the optical trap on the motion of the system is the modification of the effective mass of the particles. So, let us analyze a condensate with a time-dependent mass, moving in a parabolic trap. Since we are considering a purely classical effect we can use Gross-Pitaveskii equations (for simplicity we restrict the analysis to one dimension):

$$i\frac{\partial\psi}{\partial t} = -\frac{1}{2m}\frac{\partial^2\psi}{\partial x^2} + \frac{k}{2}x^2\psi + U|\psi^2|\psi. \tag{C1}$$

In the optical lattice the underlying equations are

$$i\frac{\partial\psi_j}{\partial t} = -J(\psi_{j+1} + \psi_{j-1}) + \frac{k}{2}j^2\psi + U|\psi^2|\psi. \tag{C2}$$

In the weak tunneling regime Eqs. (C1) and (C2) are equivalent provided that $m=1/(2J)$, the lattice constant is equal to unity, and the phase gradient is small. If the interaction strength is not too small, i.e., the condensate is in the quantum-rotor limit $UN \gg J$, then the effect of quantum pressure is negligible and instead of (C1) one can use hydrodynamic equations of motion [54]. The Bosonic field is then represented as

$$\psi(x,t) = \sqrt{\rho(x,t)}e^{i\int^x p(x',t)dx'}. \tag{C3}$$

Keeping only the lowest orders of spatial derivatives of the density ρ instead of Eq. (C1) we obtain

$$\frac{\partial p}{\partial t} = -kx - \frac{1}{m}p\frac{\partial p}{\partial x} - U\frac{\partial\rho}{\partial x}, \tag{C4}$$

$$\frac{\partial\rho}{\partial t} = -\frac{1}{m}\frac{\partial}{\partial x}(p\rho). \tag{C5}$$

The stationary solution of Eqs. (C4) and (C5) yields an inverted parabola profile of the density,

$$\rho_0(x) = \frac{\mu - \frac{1}{2}kx^2}{U}, \tag{C6}$$

where μ is the chemical potential. Let us now assume that the condensate undergoes small center-of-mass oscillations. They can be excited by a small displacement of the trap minimum. Then it is easy to check that one can seek a solution in the form

$$\rho(x,t) = \frac{\tilde{\mu}(t) - \frac{k}{2}x^2 + f(t)x}{\lambda}, \quad f(t) = -\frac{dp(t)}{dt}, \tag{C7}$$

with the initial conditions $f(0)=kx_0$, $p(0)=0$, $\mu(0)=\mu_0 - (1/2)kx_0^2$, where x_0 is the initial displacement. Substituting Eq. (C7) into Eqs. (C4) and (C5) one finds

$$f(t) = x_0 k\cos\sqrt{\frac{k}{m}}t, \quad p(t) = -x_0\sqrt{km}\sin\sqrt{\frac{k}{m}}t, \tag{C8}$$

$$\rho(x,t) = \frac{\mu - \frac{1}{2}k\left(x - \frac{f(t)}{x_0}\right)^2}{U}.$$

Note that the interaction U never enters Eq. (C8) except for a trivial prefactor. This is so because the excited mode is related to the motion of the center of mass, while the shape of the condensate cloud does not change in time. Moreover, the existence of such a center of mass or Galilean mode is the property of Eq. (C1) itself. Indeed, it is easy to check that if $\psi_0(x,t)$ is the solution of Eq. (C1) then

$$\psi(x,t) = \psi_0(x - s_0(t),t)e^{ip(t)x}e^{-(i/2)p(t)s_0(t)} \tag{C9}$$

is also a solution given that

$$\frac{ds_0}{dt} = \frac{p(t)}{m}, \quad \frac{dp(t)}{dt} = -ks_0(t). \tag{C10}$$

Now let us assume that the mass increases in time. We will use again the hydrodynamic equations (C4) and (C5), however, contrary to the stationary problem discussed above, the hydrodynamic approximation is a crucial assumption for having the center-of-mass mode independent of the interaction strength. Strictly speaking, the Galilean invariance (C9) is valid only if mass, curvature, and interaction remain constant in time. In the hydrodynamic regime the shape of the condensate does not depend on the mass, therefore we may seek a solution in a form similar to Eq. (C7):

$$\rho(t) = \frac{\mu - \frac{k}{2}\left(x - \frac{f(t)}{k}\right)^2}{U}, \quad \frac{dp}{dt} = -f(t). \tag{C11}$$

Substituting these formulas into Eqs. (C4) and (C5) yields

$$\frac{d^2p}{dt^2} + \frac{k}{m(t)}p = 0 \tag{C12}$$

which is to be supplied with the initial conditions $p(0)=0$, $\dot{p}(0)=-x_0k$. In the adiabatic limit this equation has an approximate solution:

$$p(t) \approx -x_0\sqrt{k}[m(t)m(0)]^{1/4}\sin\int_0^t \omega(\tau)d\tau, \tag{C13}$$

$$f(t) \approx x_0 k\left(\frac{m(0)}{m(t)}\right)^{1/4}\cos\int_0^t \omega(\tau)d\tau \tag{C14}$$

with $\omega(\tau)=\sqrt{k/m(\tau)}$. The first of these equations shows that as the mass increases (or equivalently the tunneling constant decreases) the momentum also increases.

[1] The special issue of Nature (London) **416**, 206 (2002).

[2] C. Orzel, A. K. Tuchman, M. L. Fenselau, M. Yasuda, and M. A. Kasevich, Science **291**, 2386 (2001).

[3] M. Greiner, O. Mandel, T. Esslinger, T. W. Hänsch, and I. Bloch, Nature (London) **415**, 39 (2002).

[4] M. P. A. Fisher, P. B. Weichman, G. Grinstein, and D. S. Fisher, Phys. Rev. B **40**, 546 (1989).

[5] D. Jaksch, C. Bruder, J. I. Cirac, C. W. Gardiner, and P. Zoller, Phys. Rev. Lett. **81**, 3108 (1998).

[6] E. Altman, W. Hofstetter, E. Demler, and M. D. Lukin, New J. Phys. **5**, 113 (2003).

[7] A. Kuklov, N. Prokof'ev, and B. Svistunov, Phys. Rev. Lett.

92, 030403 (2004).
[8] A. Kuklov, N. Prokof'ev, and B. Svistunov, Phys. Rev. Lett. **92**, 050402 (2004).
[9] M. A. Cazalilla and A. F. Ho, Phys. Rev. Lett. **91**, 150403 (2003).
[10] D.-W. Wang, M. D. Lukin, and E. Demler, cond-mat/0410494.
[11] E. Pazy and A. Vardi, cond-mat/0408269.
[12] H. P. Büchler and G. Blatter, Phys. Rev. A **69**, 063603 (2004).
[13] E. Demler and F. Zhou, Phys. Rev. Lett. **88**, 163001 (2002).
[14] O. I. Motrunich and T. Senthil, Phys. Rev. B **71**, 125102 (2005).
[15] B. Wu and Q. Niu, Phys. Rev. A **64**, 061603(R) (2001).
[16] A. Smerzi, A. Trombettoni, P. G. Kevrekidis, and A. R. Bishop, Phys. Rev. Lett. **89**, 170402 (2002).
[17] L. Fallani, L. De Sarlo, J. E. Lye, M. Modugno, R. Saers, C. Fort, and M. Inguscio, Phys. Rev. Lett. **93**, 140406 (2004).
[18] T. Anker, M. Albiez, R. Gati, S. Hunsmann, B. Eiermann, A. Trombettoni, and M. K. Oberthaler, Phys. Rev. Lett. **94**, 020403 (2005).
[19] B. Eiermann, T. Anker, M. Albiez, M. Taglieber, P. Treutlein, K. P. Marzlin, and M. K. Oberthaler, Phys. Rev. Lett. **92**, 230401 (2004).
[20] A. Trombettoni and A. Smerzi, Phys. Rev. Lett. **86**, 2353 (2001).
[21] V. A. Brazhnyi and V. V. Konotop, cond-mat/0409682.
[22] A. Polkovnikov and D.-W. Wang, Phys. Rev. Lett. **93**, 070401 (2003).
[23] J. Gea-Banacloche, A. M. Rey, G. Pupillo, C. J. Williams, and C. W. Clark, cond-mat/0410677.
[24] C. D. Fertig, K. M. O'Hara, J. H. Huckans, S. L. Rolston, W. D. Phillips, and J. V. Porto, Phys. Rev. Lett. **94**, 120403 (2005).
[25] S. Sachdev, *Quantum Phase Transitions* (Cambridge University Press, Cambridge, England, 1999).
[26] E. Altman, A. Polkovnikov, E. Demler, B. Halperin, and M. D. Lukin, cond-mat/0411047.
[27] A. Bezryadin, C. N. Lau, and M. Tinkham, Nature (London) **404**, 971 (2000).
[28] G. Schön and A. D. Zaikin, Phys. Rep. **198**, 237 (1990).
[29] W. W. Webb and R. J. Warburton, Phys. Rev. Lett. **20**, 461 (1968).
[30] J. S. Langer and V. Ambegaokar, Phys. Rev. **164**, 498 (1967).
[31] D. E. McCumber and B. Halperin, Phys. Rev. B **1**, 1054 (1970).
[32] A. Polkovnikov, E. Altman, E. Demler, B. Halperin, and M. D. Lukin, J. Supercond. **17**, 577 (2004).
[33] B. Sutherland, *Exactly Solvable Problems in Condensed Matter and Relativistic Field Theory*, Lecture Notes in Physics No. 242, edited by S. Shastry, S. S. Jha, and V. Singh (Springer, Berlin, 1985).
[34] A. R. Kolovsky and A. Buchleitner, Europhys. Lett. **68**, 632 (2004).
[35] A. Polkovnikov, S. Sachdev, and S. M. Girvin, Phys. Rev. A **66**, 053607 (2002).
[36] M. Krämer, L. Pitaevskii, and S. Stringari, Phys. Rev. Lett. **88**, 180404 (2002).
[37] J. C. Le Guillou and J. Zinn-Justin, Phys. Rev. B **21**, 3976 (1980).
[38] E. Altman and A. Auerbach, Phys. Rev. Lett. **89**, 250404 (2002).
[39] A. Georges, G. Kotliar, W. Krauth, and M. J. Rozenberg, Rev. Mod. Phys. **68**, 13 (1996).
[40] We note that within Gutzwiller approximation the size of the lattice is unimportant for finding the position of the instability as long as the number of nearest neighbors remains the same. The situation will change though, if we are interested in the time evolution of the condensate after the motion becomes unstable.
[41] A. Polkovnikov, Phys. Rev. A **68**, 033609 (2003); **68**, 053604 (2003).
[42] S. Coleman, Phys. Rev. D **15**, 2929 (1977); C. G. Callan and S. Coleman, *ibid.* **16**, 1762 (1977).
[43] C. Unger and W. Klein, Phys. Rev. B **29**, 2698 (1984).
[44] J. S. Langer, Phys. Rev. Lett. **21**, 973 (1968).
[45] J. S. Langer and M. E. Fisher, Phys. Rev. Lett. **19**, 560 (1967).
[46] A. O. Caldeira and A. J. Leggett, Physica A **121A**, 587 (1983).
[47] S. Khlebnikov, cond-mat/0502343.
[48] E. Fradkin and L. Susskind, Phys. Rev. D **17**, 2637 (1978).
[49] R. M. Bradley and S. Doniach, Phys. Rev. B **30**, 1138 (1984).
[50] B. A. Huberman, R. J. Myerson, and S. Doniach, Phys. Rev. Lett. **40**, 780 (1978); V. Ambegaokar, B. I. Halperin, D. R. Nelson, and E. D. Siggia, *ibid.* **40**, 783 (1978).
[51] P. M. Chaikin and T. C. Lubensky, *Principles of Condensed Matter Physics* (Cambridge Univesrity Press, Cambridge, England, 1995).
[52] A. Polkovnikov, cond-mat/0312144.
[53] L. De Sarlo, L. Fallani, J. E. Lye, M. Modugno, R. Saers, C. Fort, and M. Inguscio, cond-mat/0412279.
[54] V. A. Brazhnyi, A. M. Kamchatnov, and V. V. Konotop, Phys. Rev. A **68**, 035603 (2003).
[55] A. M. Rey, G. Pupillo, C. W. Clark, and C. J. Williams, cond-mat/0503477.
[56] M. Rigol, V. Rousseau, R. T. Scalettar, and R. R. P. Singh, cond-mat/0503302.